



Global Physics Performance at the Ref-TDR

Chenguang Zhang



中國科學院高能物理研究所
Institute of High Energy Physics
Chinese Academy of Sciences

Jun 17th, 2025, Barcelona

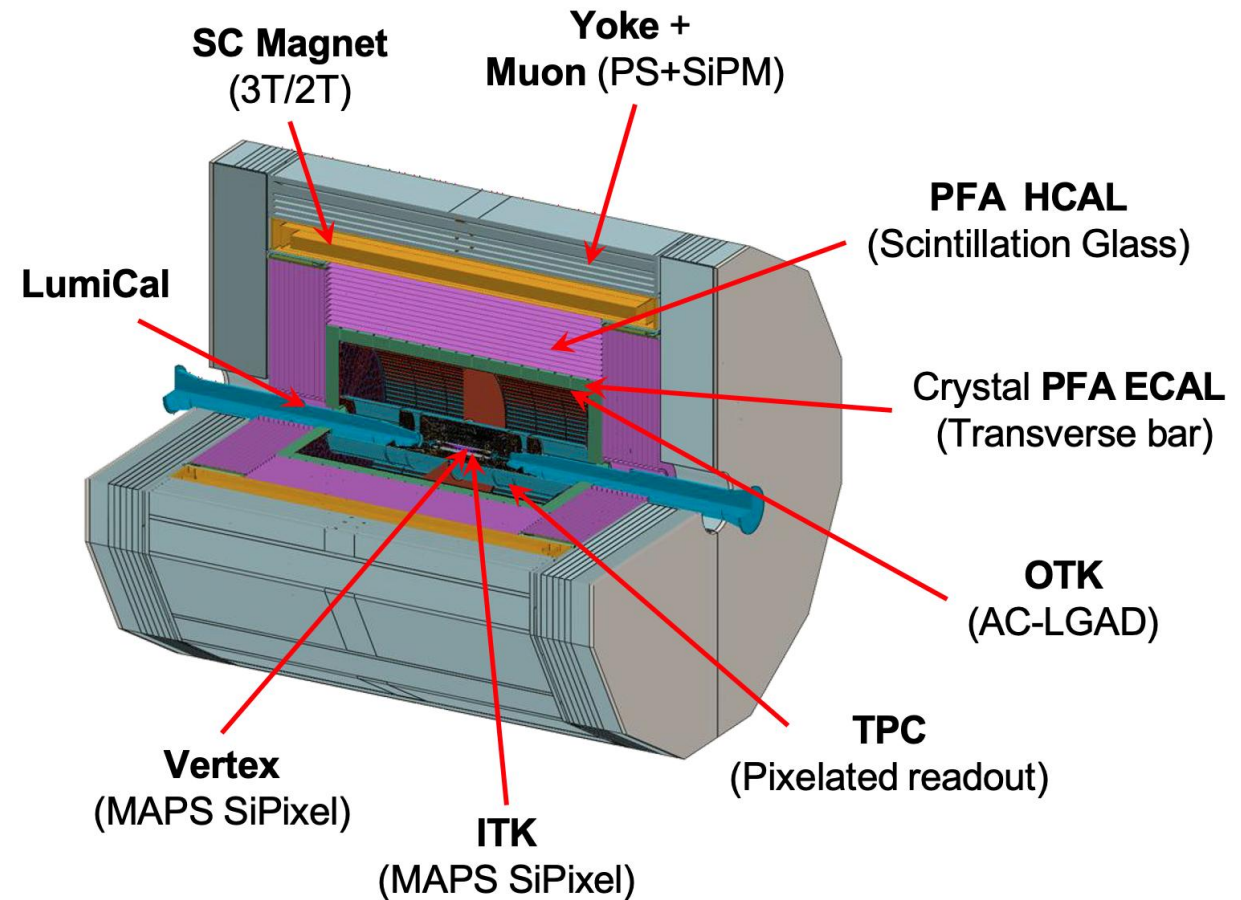
Content

- **Introduction**
- **Tracking**
- **Particle identification**
- **Vertexing**
- **Jet**
- **Missing energy, momentum, mass**

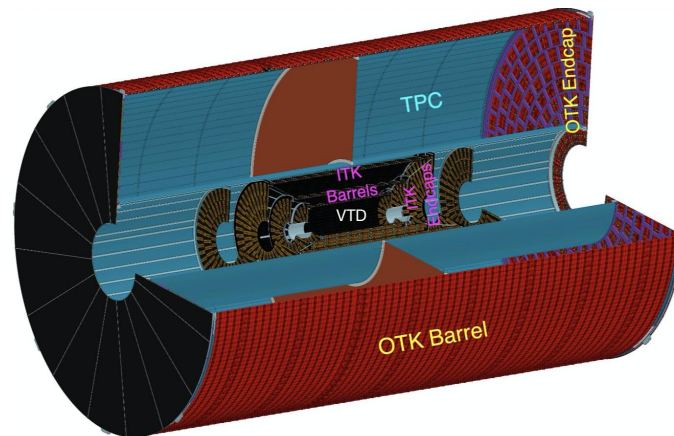
Introduction

PFA is essential for the majority of physics

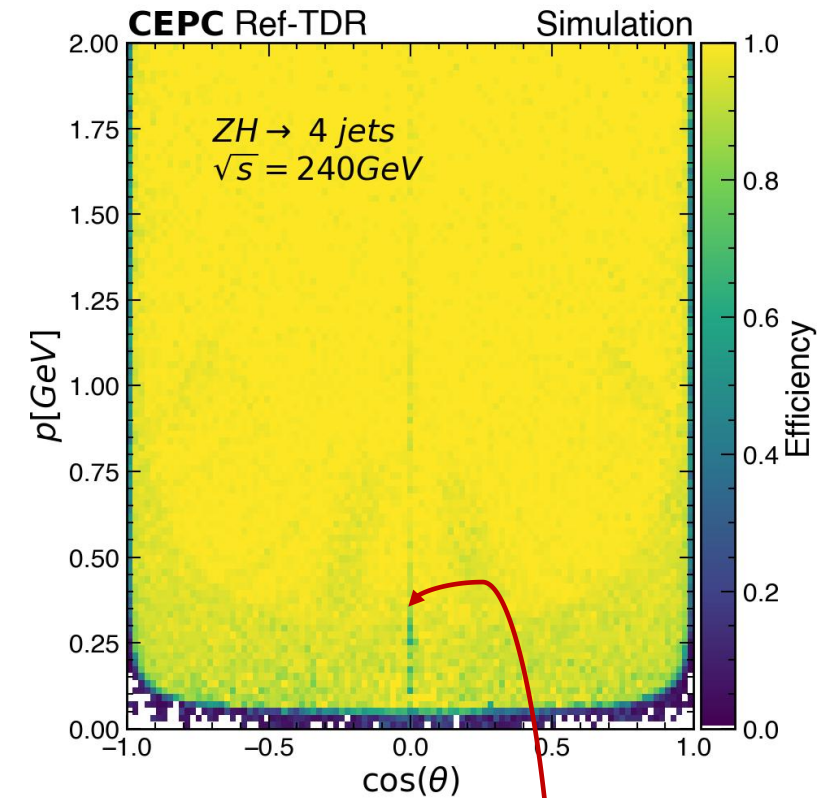
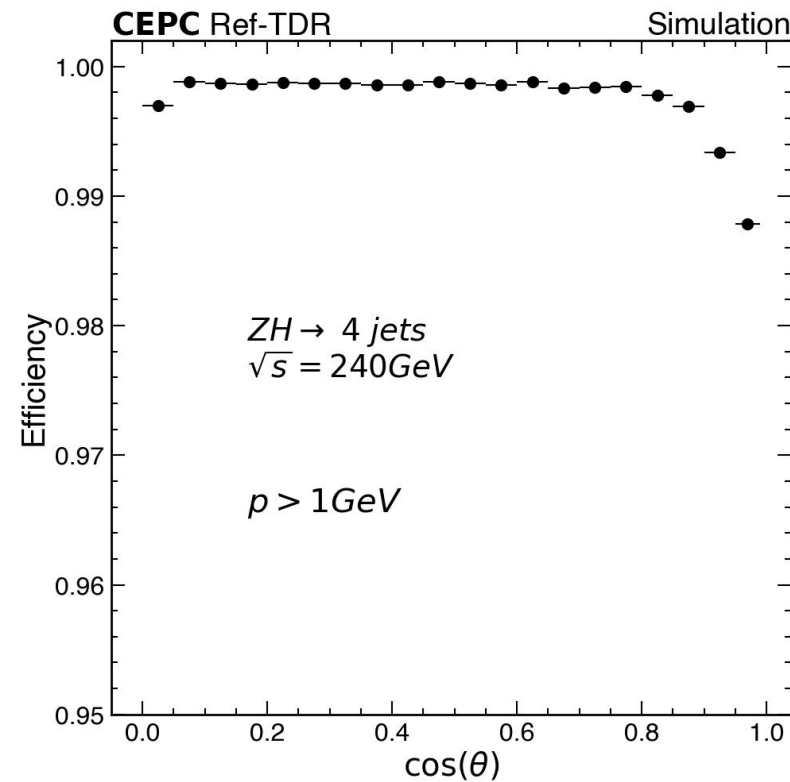
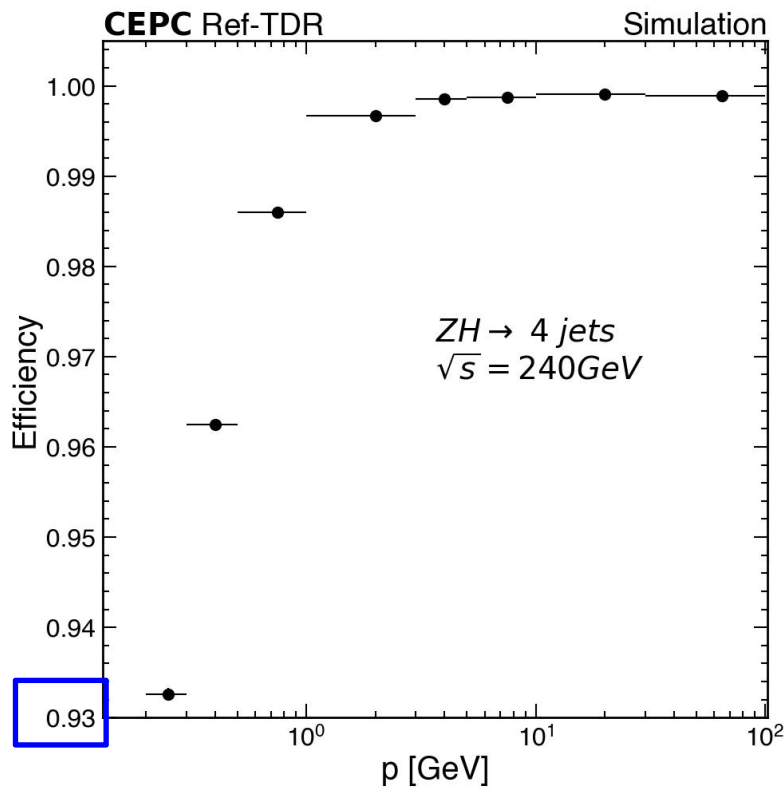
- Tracking efficiency: Nearly 100%
- Tracking momentum resolution: $\sim 0.1\%$
- VTX: position resolution $\sim 5 \mu\text{m}$
- EM resolution: $\sim 1\%$
- Particle Identification (PID): $> 3\sigma$ separation between π and k for $P < \sim 20$ GeV
- Boson Mass Resolution (BMR): $< 4\%$



Tracking



Tracking efficiencies



- For the combined tracking system, reconstruction efficiency is on average 99.7% for tracks with $p > 1 \text{ GeV}$
- The membrane cathode spanned between two rings in the center of the TPC causes some inefficiency
- The impacts from beam-induced background has been studied and found to be negligible

Tracking momentum resolution

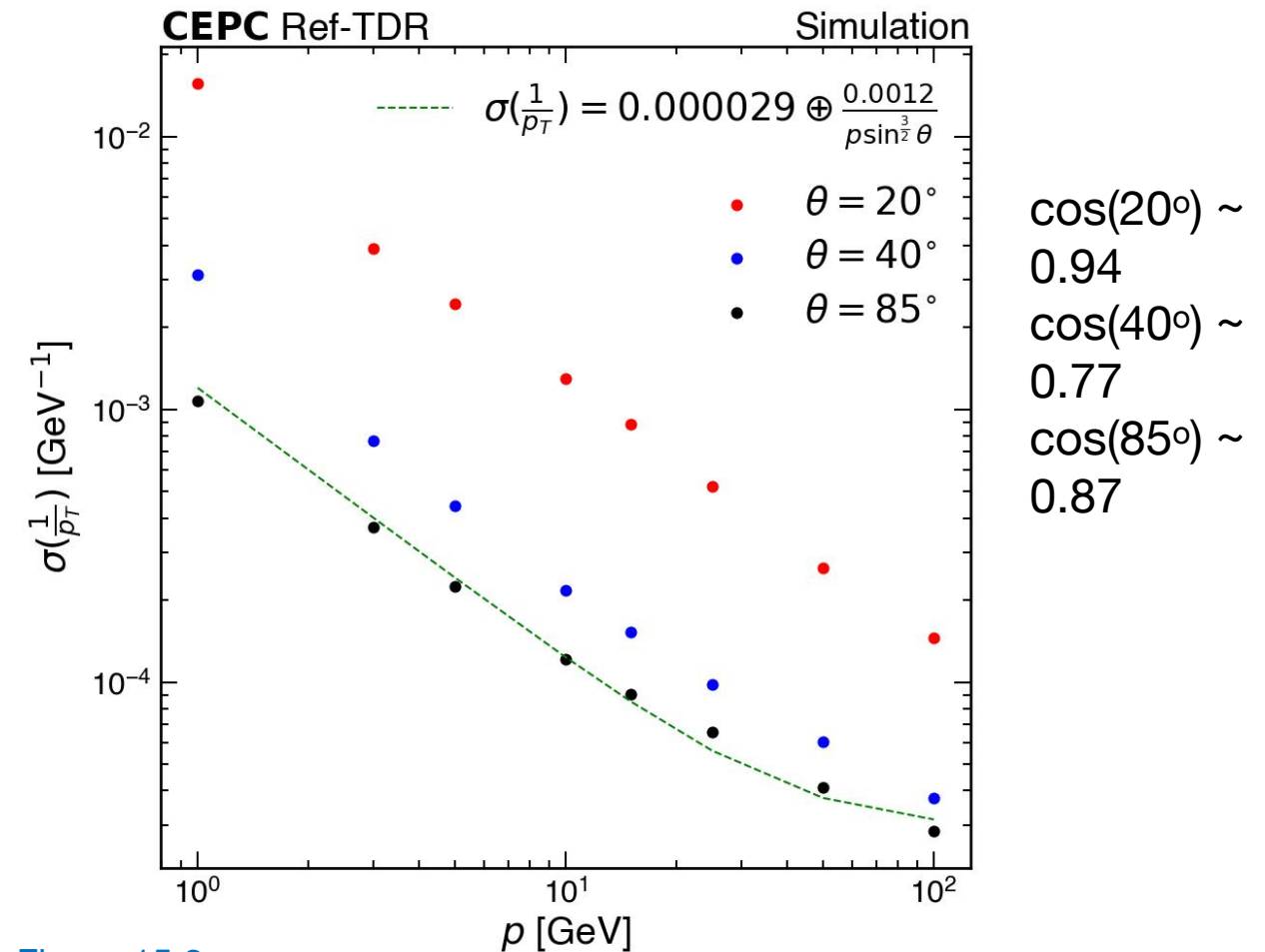
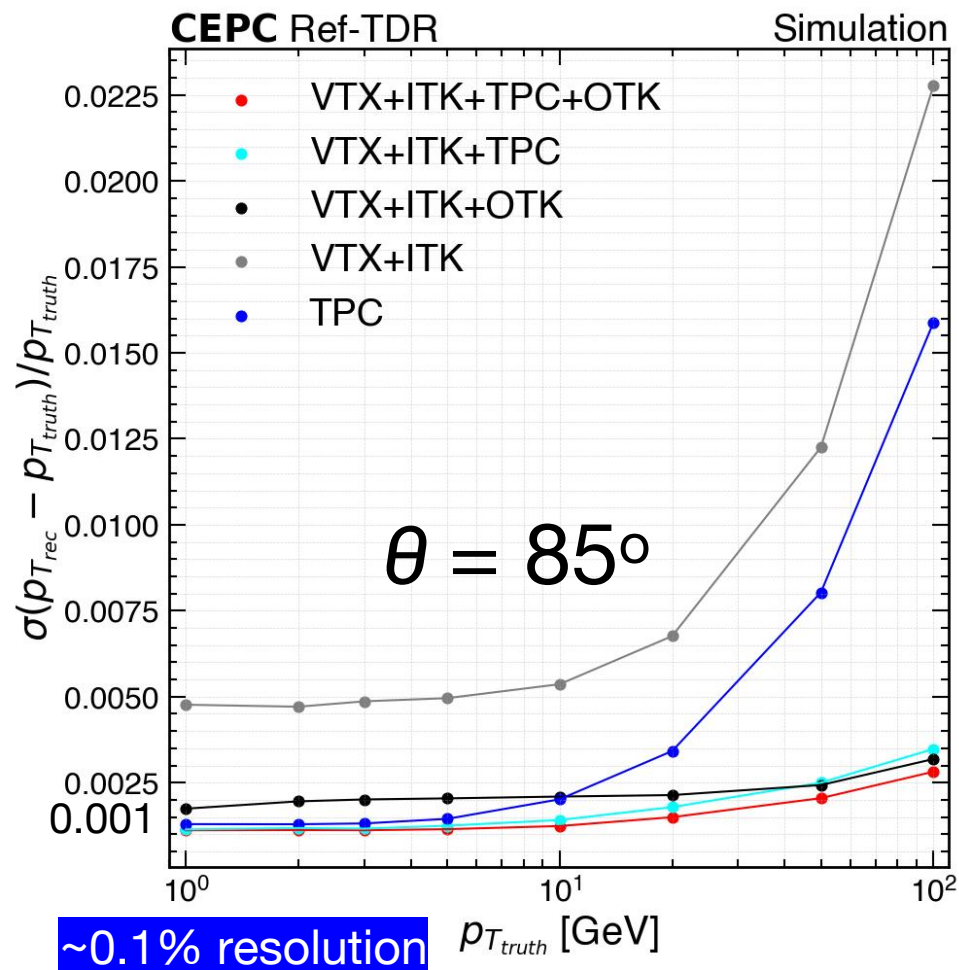


Figure 15.3

- TPC helps improve the resolution significantly at low momentum region
- Both TPC and OTK are able to help improve the resolution at high momentum region

Impact parameter resolution

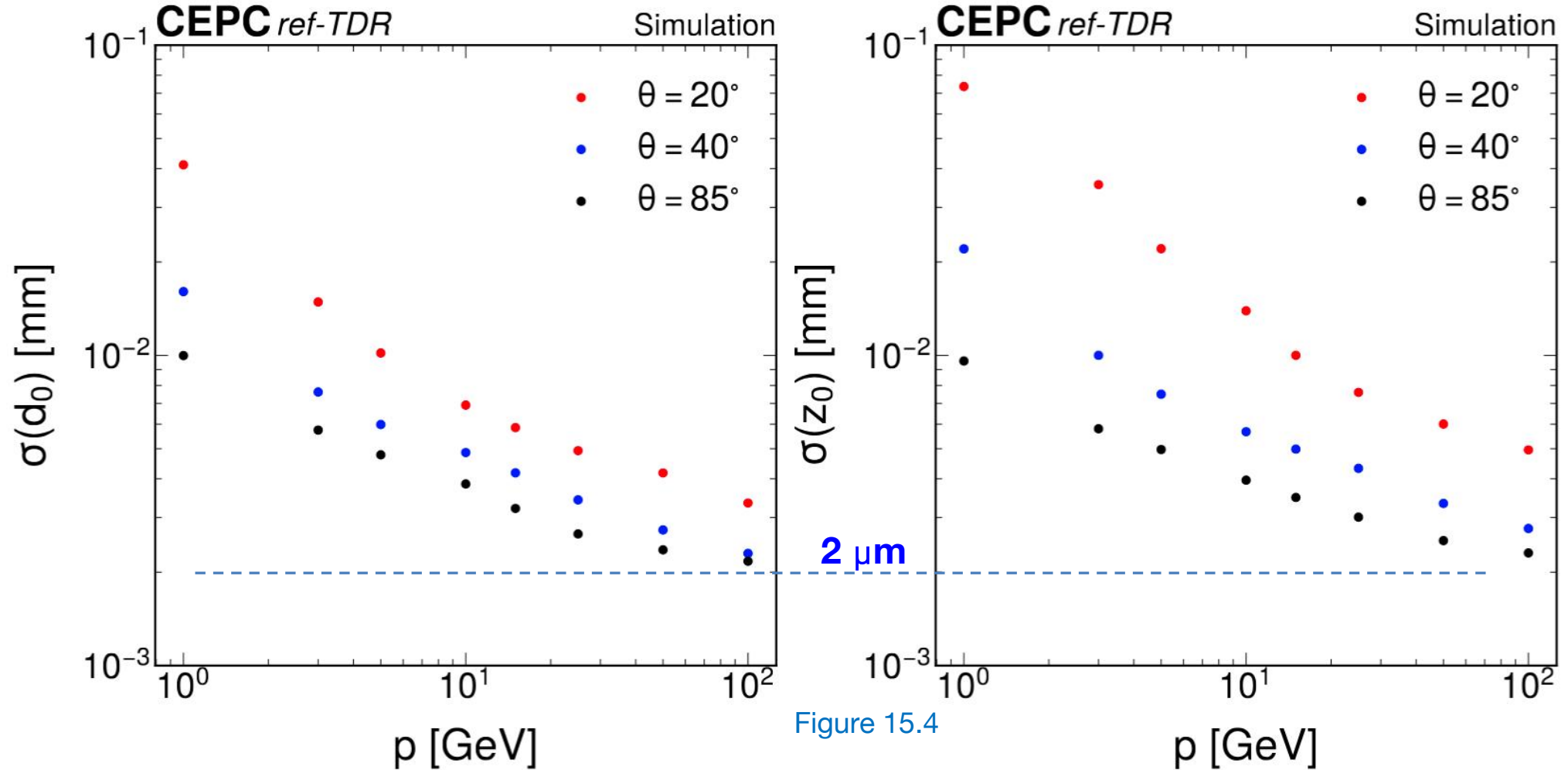


Figure 15.4

- Both d_0 and Z_0 resolutions are excellent, reaching 2-3 μm for the whole barrel region for $p > 50$ GeV

PID

TPC, TOF for charged hadrons
ECAL, HCAL, Muon Detector for
lepton/photon

Lepton ID

- XGBoost:** dN/dx , TOF, E_{ECAL} , E_{HCAL} , I_{HCAL} and ΔR between track and hits in muon system; + few more variables [see backup]

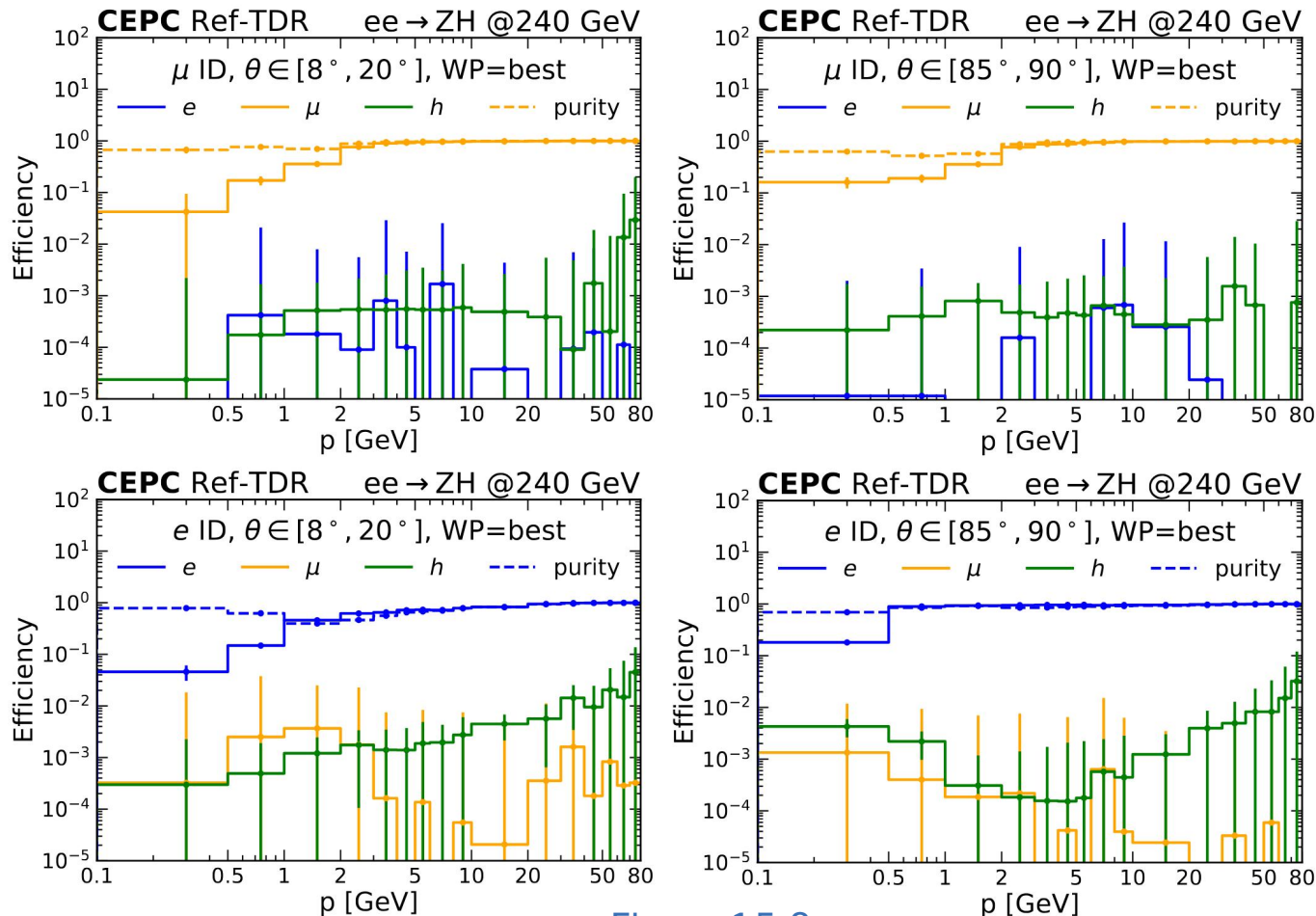


Figure 15.8

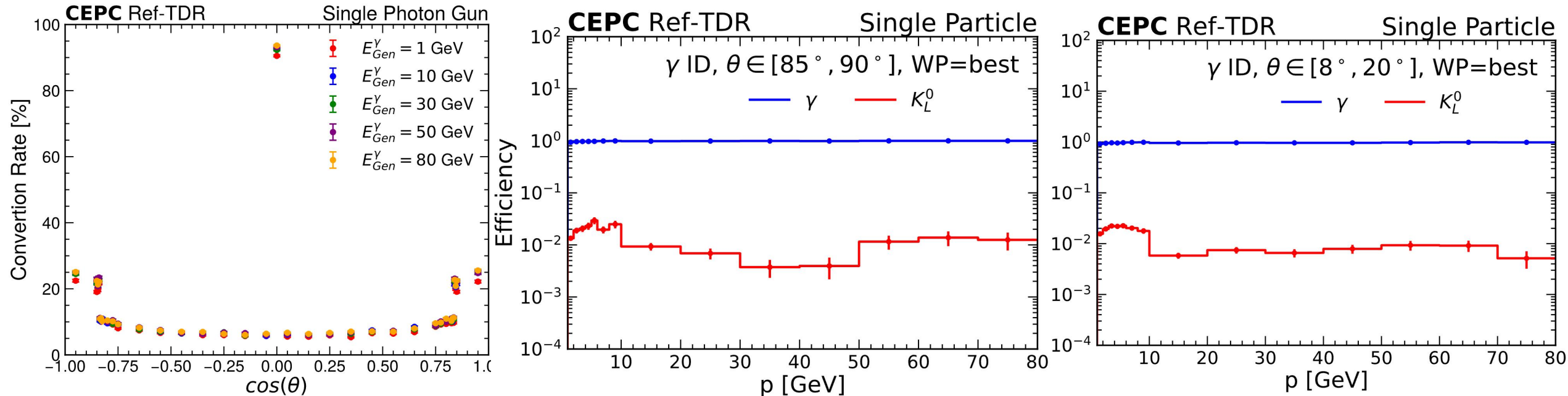
muon ID:

- Efficiency falls below 50% for momentum less than 2 GeV
- As momentum surpass 2 GeV, efficiency approaching 100% rapidly
- Mis-id rate for electrons and charged hadrons is around 0.1% or lower

electron ID:

- The global performance is similar with muon ID
- mis-identification from charged hadron is higher peaking at approximately 1% at high momenta
- The purity of both electron and muon is predominantly above 90%

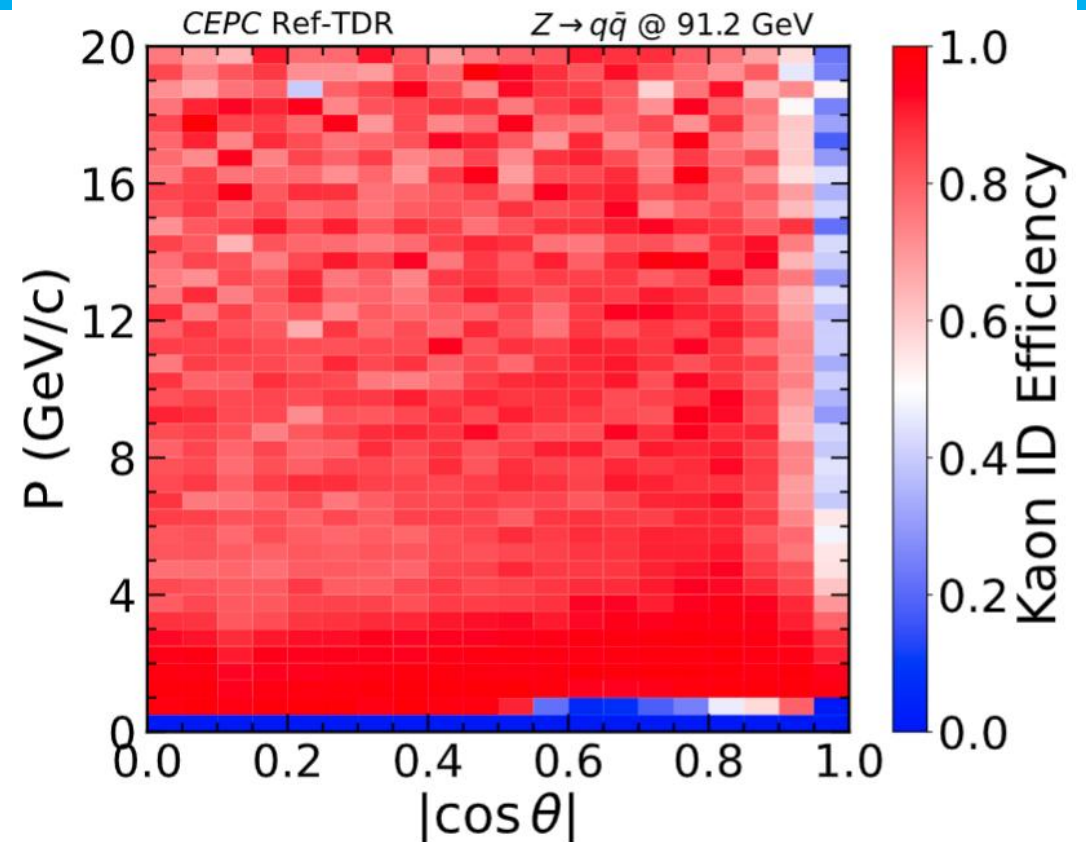
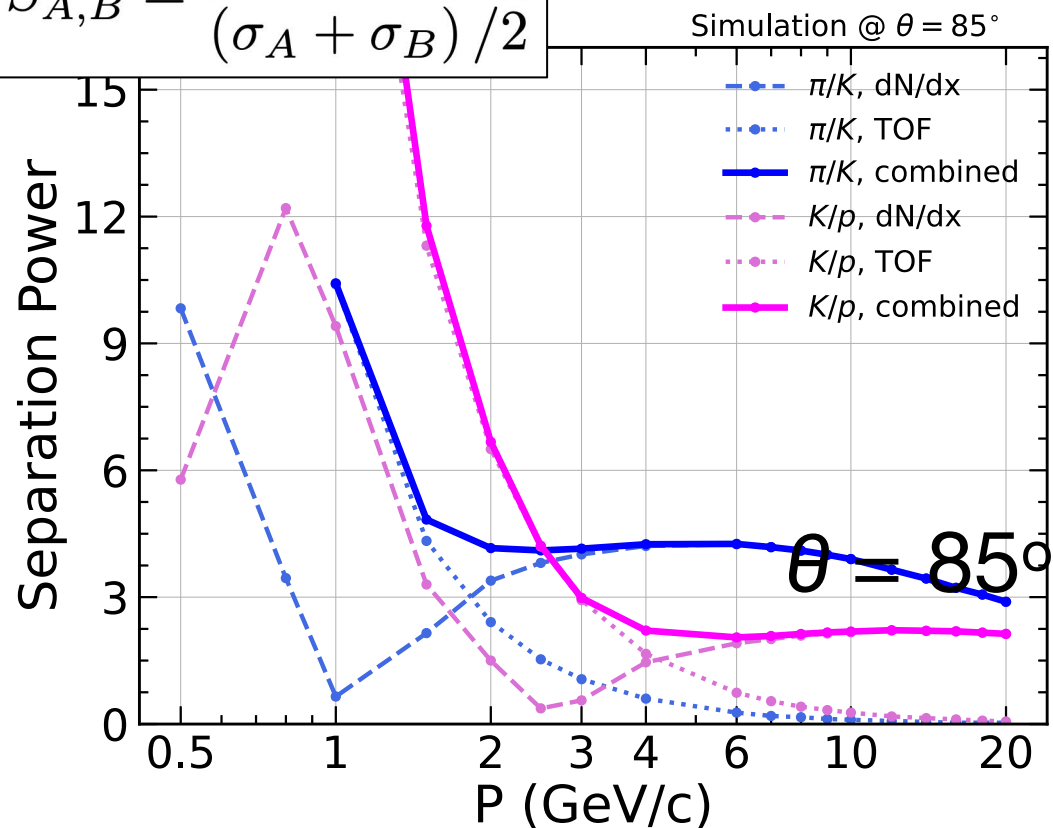
Photon Identification



- 6-10% of photons in the central region and 25% of photons in the forward region convert to electron pairs
- For un-converted photons with energy above 3GeV, their reconstruction efficiency reaches 100%. The photon energy resolution is excellent in 1-100 GeV range [see PFA talks]
- Un-converted photons need to be identified from neutral hadrons, which are pre-dominantly K-long. Similar to Lepton ID, an XGboost-based algorithm is exploited
 - photon ID efficiency is stable above 90% and approaching 100%
 - K-long mis-ID rate is around 2% at $p < 10$ GeV and 1% at $p > 10$ GeV

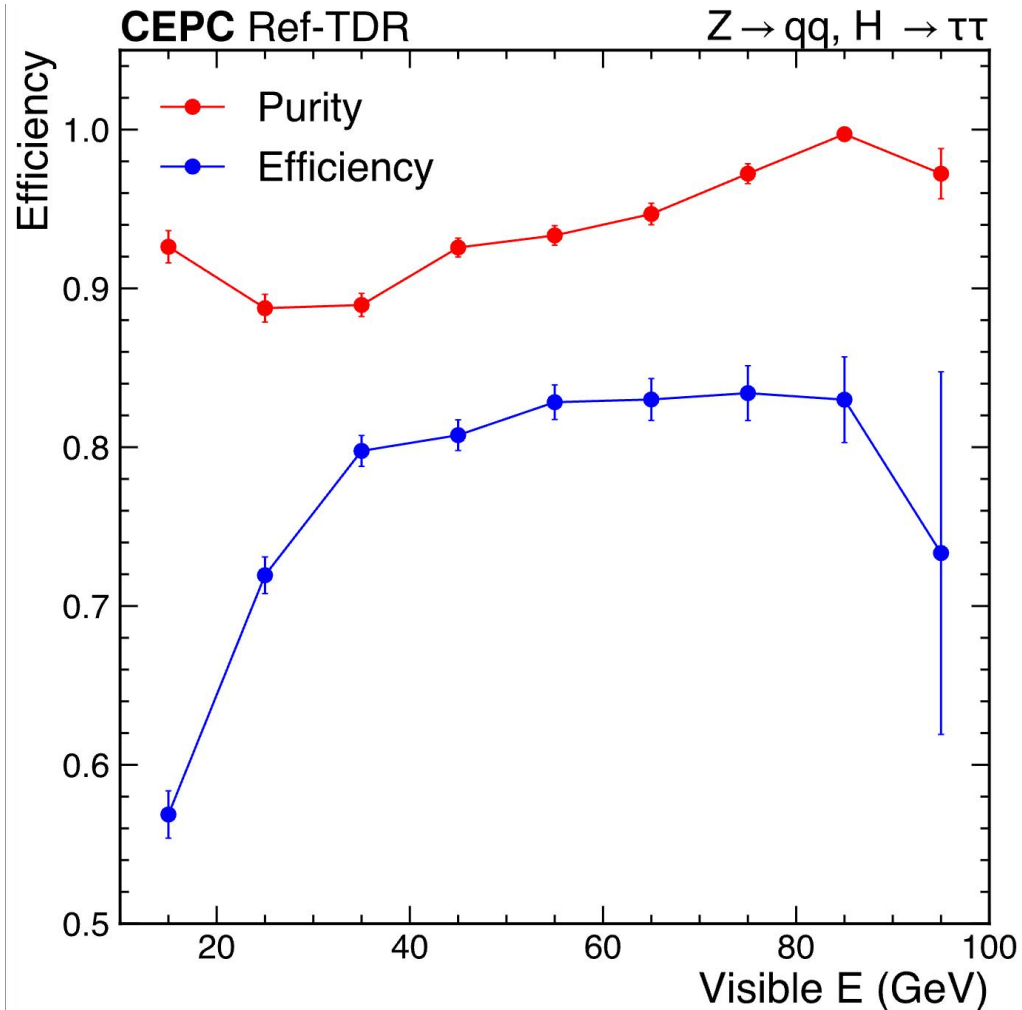
Charged Hadron PID

$$S_{A,B} = \frac{|\mu_A - \mu_B|}{(\sigma_A + \sigma_B)/2}$$



- Charged hadron PID can be evaluated by XGboost-based algorithm as well. Because the K/pi/proton separation is primarily determined/limited by TPC and TOF, there is a dedicated discussion for clear understanding
- K/pi separation power achieves 3 sigma in 1-20 GeV**
- Particles with $p < 1$ GeV in barrel region rarely reach TOF**
- Particles with $p < 0.5$ GeV in barrel region, also difficult to be reconstructed in TPC**

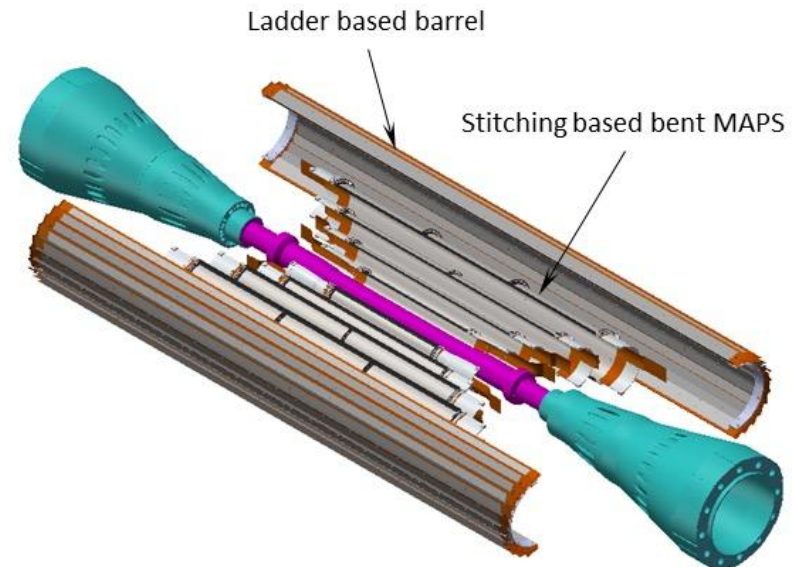
Tau-lepton identification



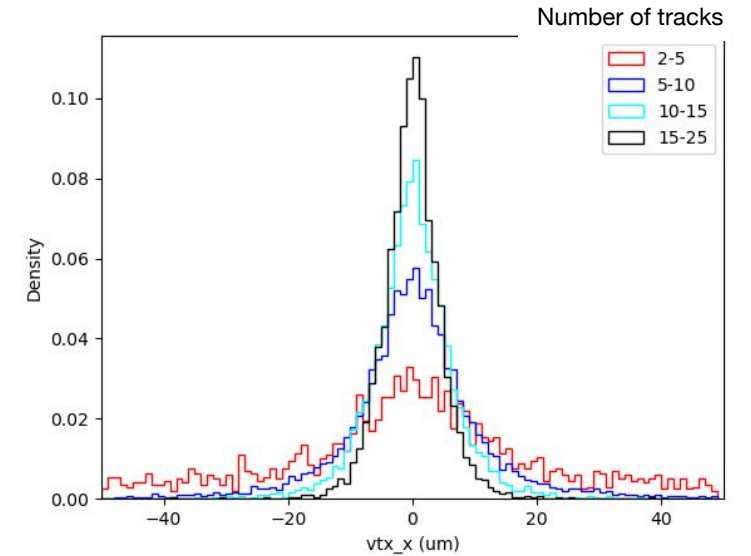
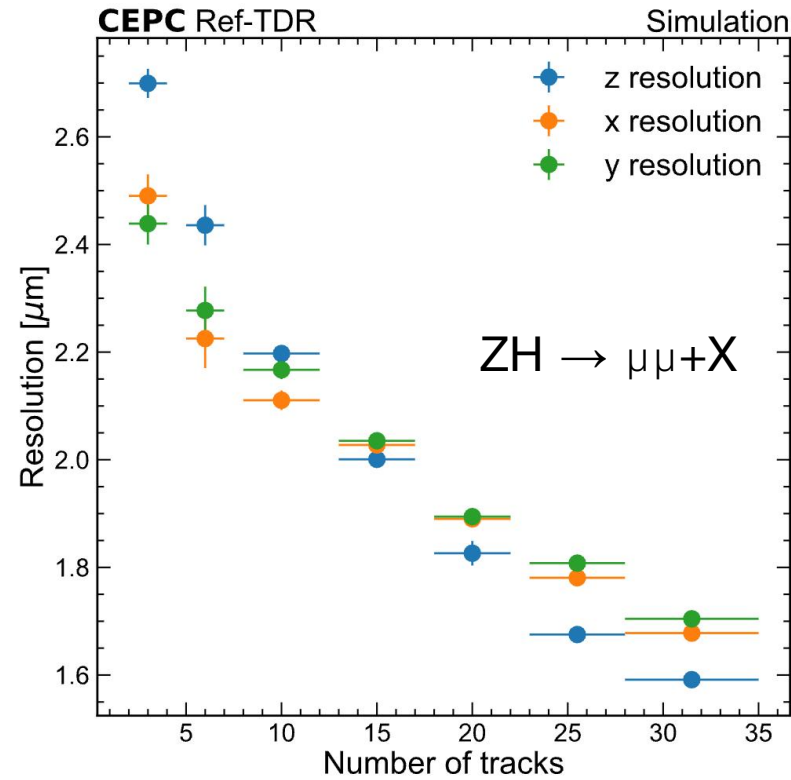
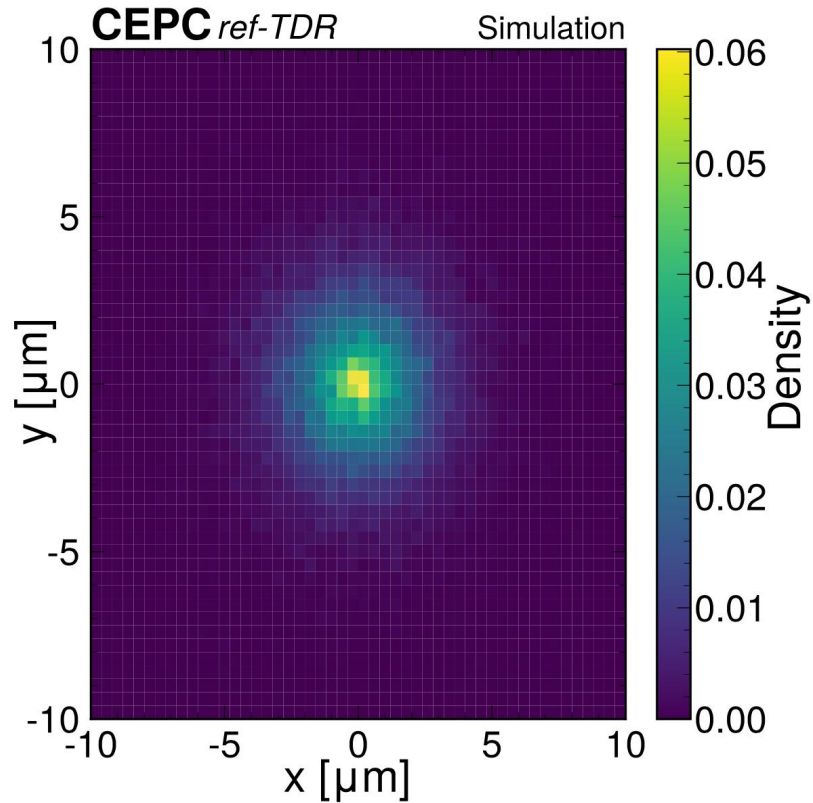
- Hadronic decays of tau leptons appear in the detector as narrow jets with a low multiplicity of particles. An initial tau-lepton identification algorithm has been devised
 - Starting from a seed track whose energy exceeds 1.5 GeV, and gather charged and neutral particles within a small cone of 0.12 radians to form a tau-lepton candidate
 - Primary backgrounds, from hadronic jets, are removed by cuts on invariant mass and isolation
- The efficiency and purity as functions of the visible energy of tau candidate from 10-100 GeV
 - Efficiency approaches 80%
 - Purity surpasses 90%

A similar algorithm following LCFIPlus has been developed

Vertexing

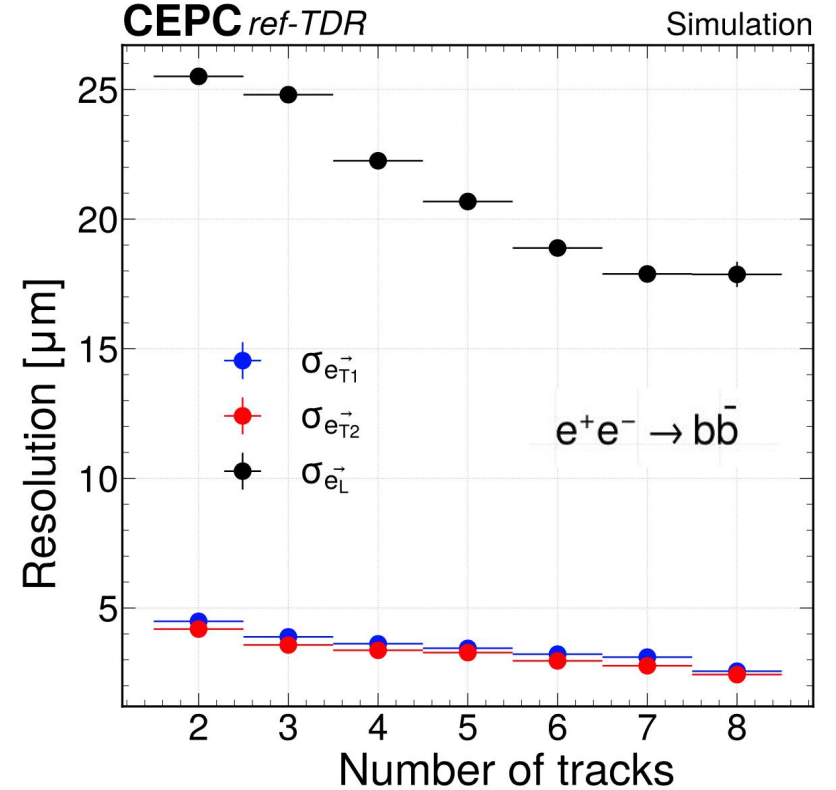
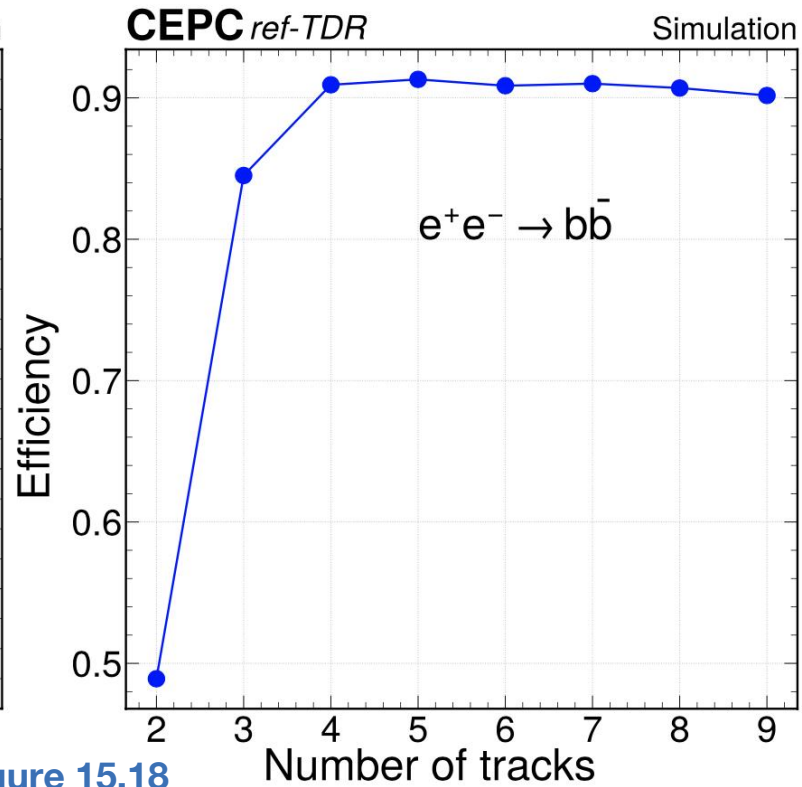
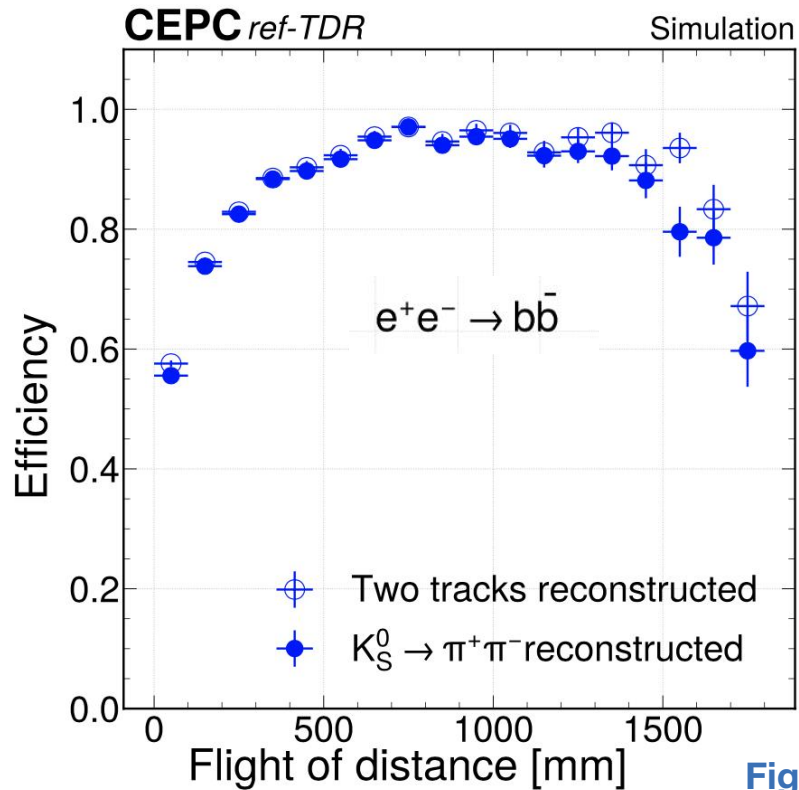


Primary Vertex



- Excellent resolution as expected, $< 3 \mu\text{m}$ for low multiplicity events, and $< 2 \mu\text{m}$ for high multiplicity events.

Secondary vertex



- With $ee \rightarrow bb$ sample, the average efficiency for Ks is ~70%
- The efficiency for all true secondary vertices is ~75%
 - A true secondary vertex is considered reconstructed if a reconstructed secondary vertex is found within a distance of 200 μm
 - if a true vertex with > 2 tracks, at least two corresponding reconstructed tracks must be used to form this reconstructed vertex
- Excellent resolution for secondary vertex

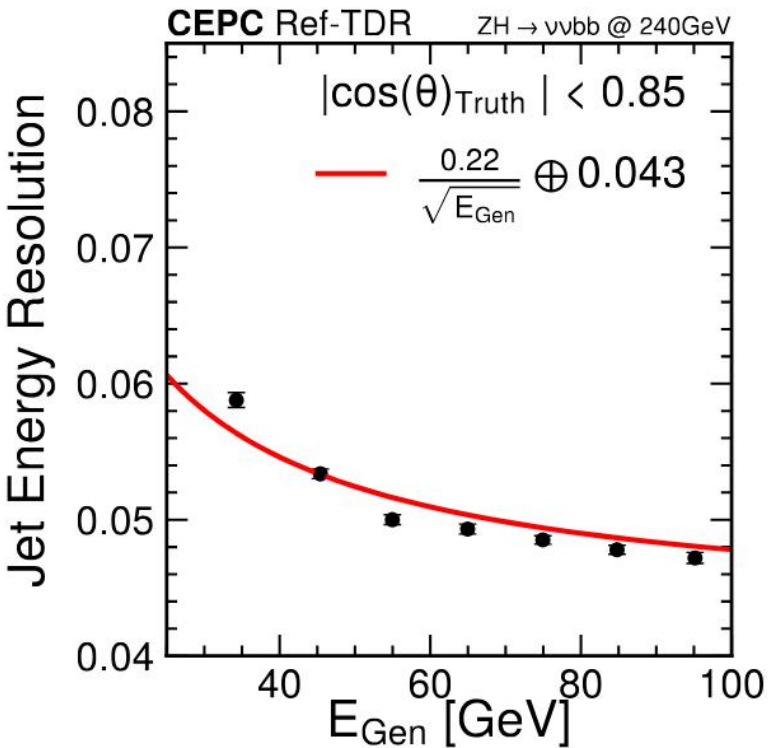
Figure 15.20: Resolution of the transverse and longitudinal components of the secondary vertices

Jets

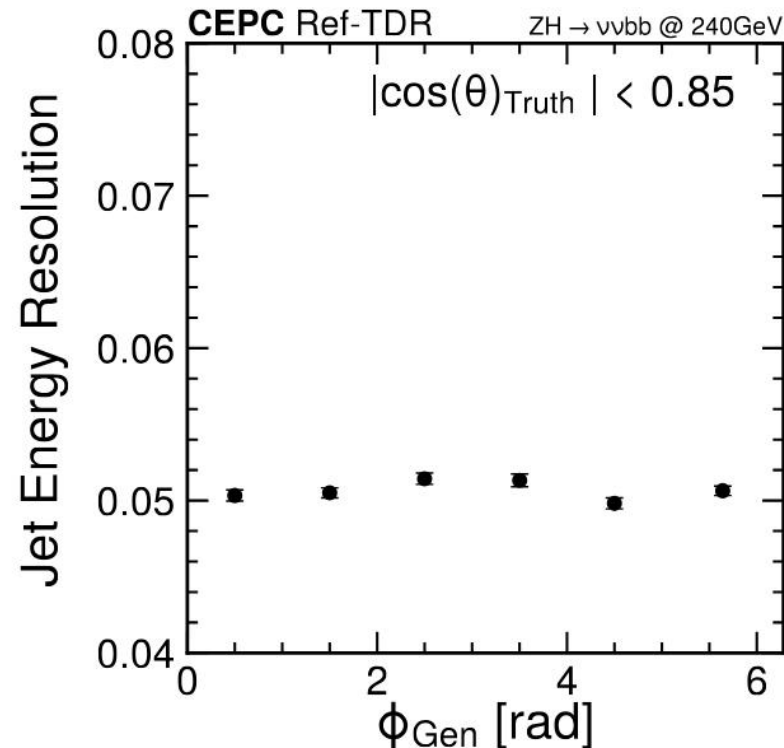
Jets are reconstructed using ee-kt algorithm with FastJet package, based on PFO objects reconstructed by **CyberPFA***

*CyberPFA described in the report of software group

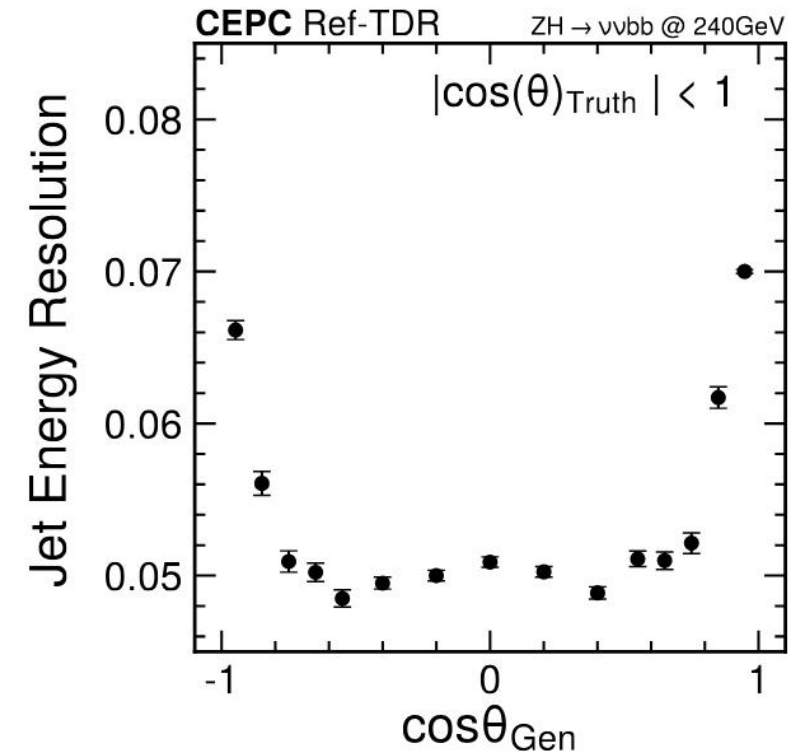
JER



JER vs E



JER vs ϕ

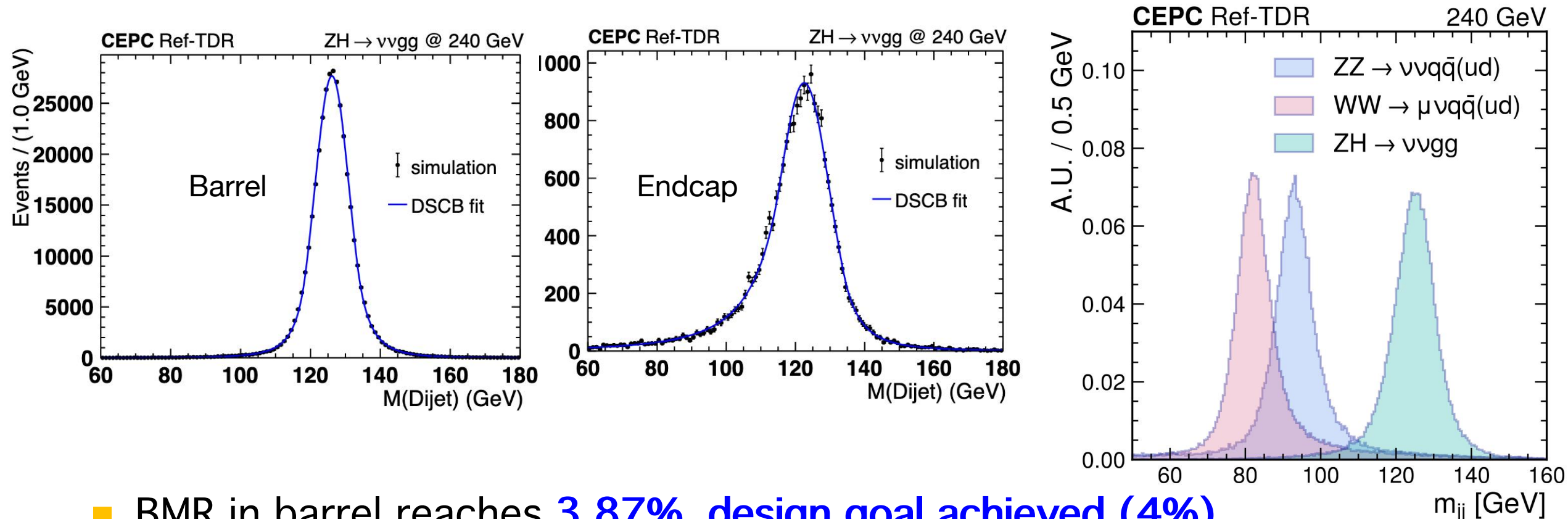


JER vs $\cos\theta$

- ~5% in the barrel region, slightly worse in the endcap

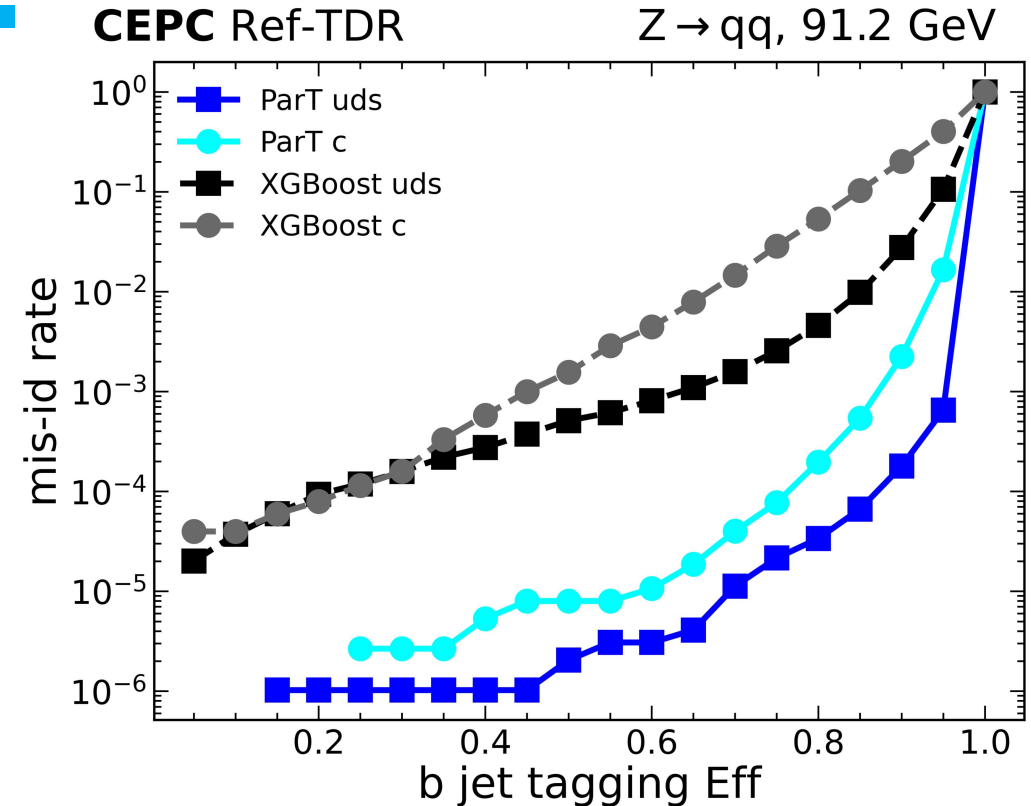
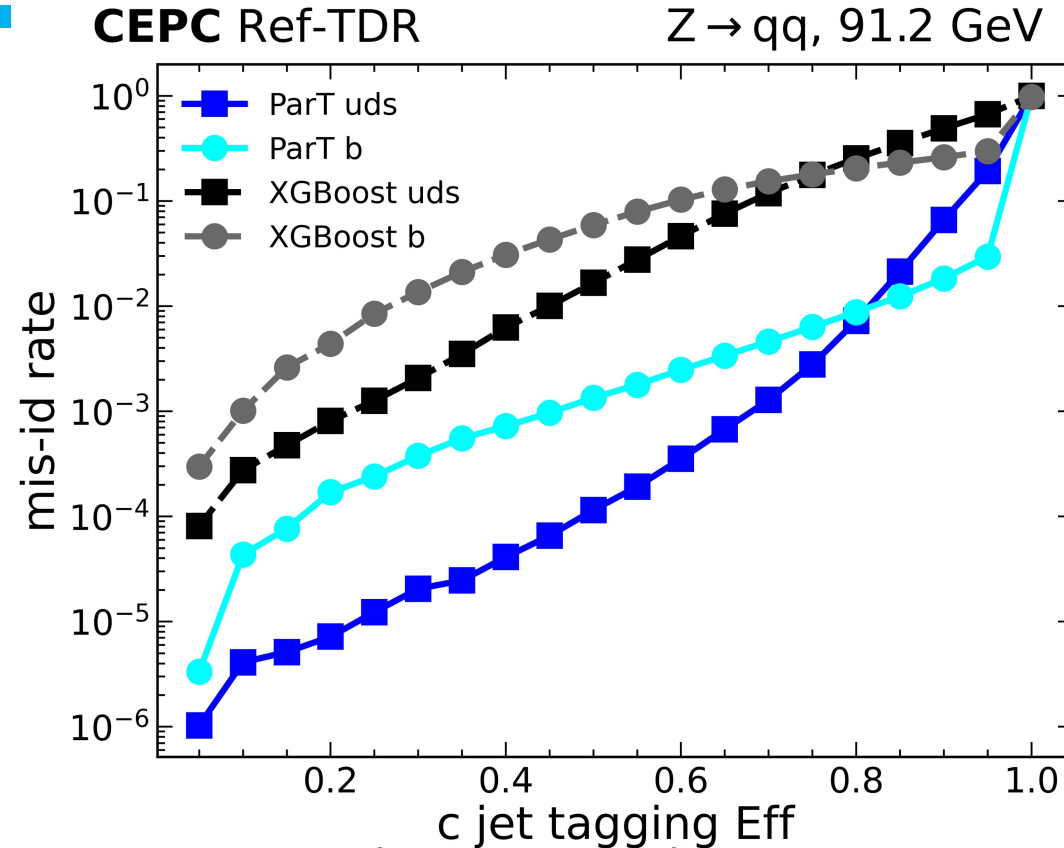
Boson Mass Resolution

No cleaning of events here, i.e. no requirement on energy sum of ISR, or neutrinos



- BMR in barrel reaches **3.87%**, design goal achieved (4%)
- ~ 6% in the endcap region

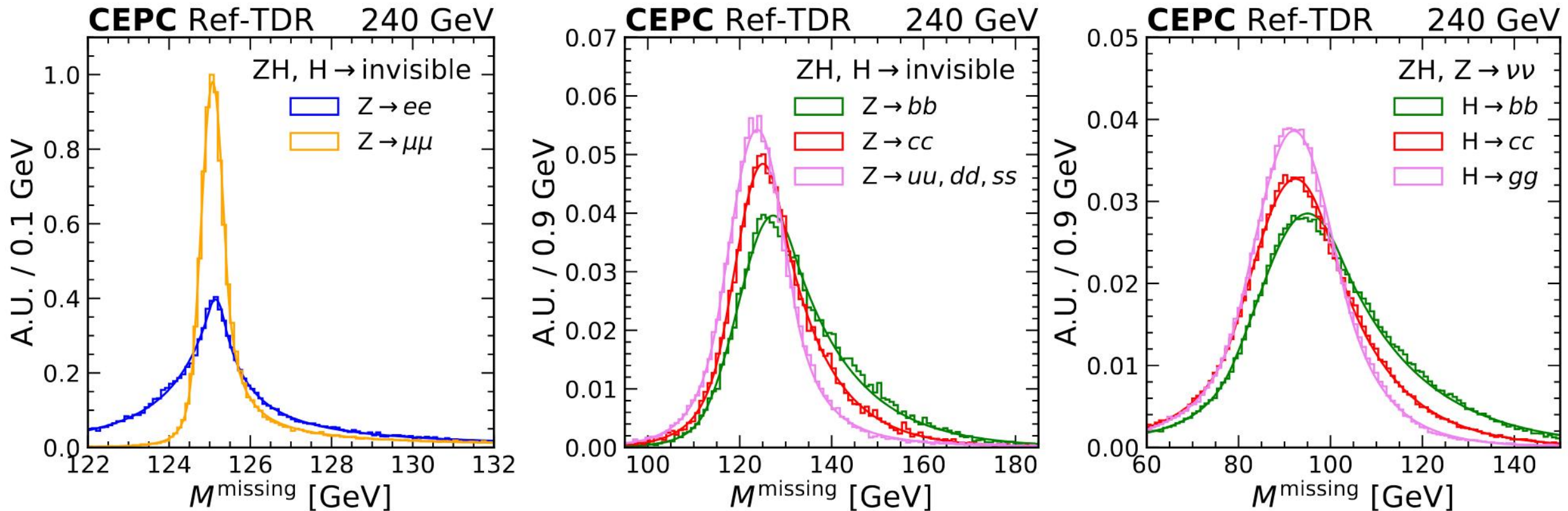
Jet Flavor Tagging



- XGBoost and JOI(Jet Origin ID) are tested based on Ref-TDR with Z to qq events
- For XGBoost
 - b tagging: misID rates at $\epsilon_{b\text{-jet}} = 80\%$ (50%) are **2.23%** (**0.11%**) for c-jets and **0.24%** (**0.03%**) for uds-jets.
 - c tagging: misID rates at $\epsilon_{c\text{-jet}} = 80\%$ (50%) are **13.58%** (**2.87%**) for b-jets and **13.9%** (**0.78%**) for uds-jets.
- JOI performance is about 1-2 order of magnitude better than XGBoost
 - Remarkably, **b-jet efficiency $\sim 95\%$ with mis-id rate of only 0.1%** from light quark jets

Missing energy, momentum, mass

Missing energy, momentum, mass



- The effects from neutrinos are demonstrated at Higgsstrahlung events
- **Z to mu mu has the best missing mass resolution of 0.288 GeV; Z to ee has a slightly worse resolution of 0.40 GeV**
- **For 2-jet events, 6.4 GeV for Z to light quarks, H to 4v; 9.2 GeV for Z to vv, H to gg**

Summary

- Physics object performance through full simulation shown

- Tracking p_T resolution $\sim 0.1\%$ achieved for majority
- PID (TPC+TOF) $\sim 3\sigma$ separation power for 1-20 GeV π -k
- Sub-percent EM resolution
- BMR reaches the design goal: $\sim 3.87\%$ for H- \rightarrow gg
- Excellent vertex performance: <3 mm for x/y/z resolution

Tracking eff	Tracking σ_{pT}	VTX $\sigma_{x,y,z}$	π -k separation	EM resolution	BMR
>99.7% (for $p>1$ GeV)	$\sim 0.1\%$	$< 3 \mu\text{m}$	3σ (1-20 GeV)	$1.5\%/\sqrt{E}$ $\oplus 0.25\%$	3.87% (H- \rightarrow gg)

all the requirements

- Some physics benchmark studies [see other talks]

- **Excellent precision on various observables**

- Work towards TDR publication

- Finish the benchmark studies, in particular for systematic uncertainties

- Work beyond TDR

- GSF fitting of electron, reconstruction of standalone muon, CyberPFA optimization ...
- Further optimizing detector configuration through physics performance studies



**Thank you for your
attention!**



中國科學院高能物理研究所
Institute of High Energy Physics
Chinese Academy of Sciences

April 14-16, 2025, CEPC Detector Ref-TDR Review

Backup

CEPC physics

Chinese Physics C Vol. 43, No. 4 (2019) 043002

Precision Higgs physics at the CEPC*

Fanfan An安芬芬^{1,2}, Yu Bai白钰¹, Chuan Chen陈春梅^{1,3}, Xin Chen陈鑫¹, Zhenzhen Chen陈真真^{1,4}, Jun Guo郭俊^{1,5}, Zhenwei Guo郭震威¹, Yuesha Jiang姜亚莎^{1,6,7}, Changsheng Jia贾长胜¹, Jun Guo郭俊^{1,5}, Yuesha Jiang姜亚莎^{1,6,7}, Xiaoming Guo郭晓明¹, Shuang Guo郭双^{1,8}, Jinyu Guo郭锦宇^{1,9}, Fugang Guo郭富强¹, An Guo郭安¹, Tao Han韩涛¹⁰, Shuang Han韩爽¹, Hongjun He何红建^{11,12}, Xinda He何佳琪¹³, Xiaoping He何小桐^{14,15}, Jidong He何继峰¹⁶, Shaohua He何少华¹⁷, Sha Jiang姜召¹, Mingqiang Jiang蒋鸣强¹⁸, Siyuan Jiyedelman¹⁹, Ruyun Kang康睿¹, Chao-Ming Kao高家庆²⁰, Peihua Lai赖佩华²¹, Boyang Lai李博洋²², Congqiao Li李聪桥²³, Gang Li李刚^{14,15}, Haidong Li李海峰²⁴, Liang Li李亮¹, Siu Li李秀^{1,25}, Tong Li李通^{1,26}, Qiang Li李强¹, Hui Liang梁惠¹, Zhenjun Long梁志远²⁷, Libo Luo罗立波²⁸, Bo Luo罗博²⁹, Jiamel Luo罗健³⁰, Tao Luo罗涛³¹, Zhen Liu刘震^{32,33}, Xuebin Luo罗雪彬^{34,35}, Lianhua Mei梅连华³⁶, Binuo Miao苗彬³⁷, Xin Mo莫欣³⁸, Mile Prandrova³⁹, Jianming Qian钱建明⁴⁰, Zhousi Qian钱思琦⁴¹, Nikoloz Rongpeti⁴², Mengyuan Song孙梦园⁴³, Alex Schryer⁴⁴, Langyuan Shan申亮远⁴⁵, Jingyuan Shi史敬远⁴⁶, Xia Sha沙夏⁴⁷, Shuang Shi史双⁴⁸, Dayong Wang王大为⁴⁹, Yu Wang王宇⁵⁰, Lianhua Wang王连华⁵¹, Yiding Wang王懿芳⁵², Yongjun Wei魏永军⁵³, Yue Xu徐悦⁵⁴, Huijun Yang杨辉军⁵⁵, Yinyi Yang杨依依⁵⁶, Weiming Yao姚伟民⁵⁷, Duo Yue于多⁵⁸, Kai Zhang张凯⁵⁹, Zhenyu Zhang张振宇⁶⁰, Mingzi Zhao赵明子⁶¹, Xianjun Zhao赵贤俊⁶², Ming Zhang张明⁶³

Higgs White Paper (2019) 4, 043002

Higgs

m_H, σ, Γ_H

self-coupling

$H \rightarrow bb, cc, ss, gg$

$H \rightarrow inv, H \rightarrow sb, \dots$

Flavor

CKM matrix

CPV measurements

LFV, LUV

τ properties (lifetime, BRs..)

$B_c \rightarrow \tau \nu, B_s \rightarrow D_s K/\pi$

$B_s \rightarrow K^* \tau \tau, B \rightarrow K^* \nu \nu$

$B_s \rightarrow \phi \nu \nu \dots$

Top

$m_{top}, \Gamma_{top},$

top quark coupling,

...

~ 4.3 million Higgs

~ 4 trillion Z bosons

~ 400 million W pairs

~ 600 k ttbar

EWK/QCD

$m_Z, \Gamma_Z, \Gamma_{inv}$

$\sin^2\theta_W, m_W, \Gamma_W,$

$A_{FB}^{b,c}, \tau$ pol.

α_S, \dots

BSM

Heavy Neutral Leptons

Dark Photons Z_D

Axion Like Particles

Exotic Higgs decays

...

Flavor Physics at CEPC: a General Perspective

Contents

1 Introduction	2
2 Description of the CEPC Facility	6
2.1 Key Collider Features for Flavor Physics	6
2.2 Key Detector Features for Flavor Physics	7
2.3 Simulation Method	16
3 Charged Current Semileptonic and Leptonic b Decays	17
4 Rare/Penguin and Forbidden b Decays	21
4.1 Dilution Modes	23
4.2 Neutrino Modes	25
4.3 Radiative Modes	27
5 CP Asymmetry in b Decays	27
6 Global Symmetry Tests in Z and b Decays	32
7 Charm and Strange Physics	35
7.1 Null tests with rare charm decays	36
8 τ Physics	36
8.1 LFV τ Decays	37
8.2 LFU Tests in τ Decays	38
8.3 Hadronic τ Decays and Other Opportunities	40
8.4 CPV in Hadronic τ decays	41
9 Exclusive Hadronic Z Decays	42
10 Flavor Physics beyond Z Pole	43
10.1 V_{cb} and W Decays	43
10.2 Top FCNC	45
11 Spectroscopy and Exotics	46
12 Light BSM States from Heavy Flavors	50
12.1 Lepton Sector	51
12.2 Quark Sector	51

Flavor White Paper, summarizing ~ 40 benchmarks, submitted

- Physics merit quantified by simulation & phenomenology studies:
 - Higgs Physics:** precisions exceed HL-LHC by ~ one order of magnitude
 - EW Studies:** precision improved by one to two orders of magnitude over current existing results
 - Flavor Physics:** sensitive to new physics at energy scales of 10 TeV or higher
 - BSM physics:** sensitivity to a variety of potential signals

CEPC Detector Requirements

Excellent tracking resolution/
Jet energy resolution
Impact parameter resolution for b,c,s tagging

Higgs
 m_H, σ, Γ_H
 self-coupling
 $H \rightarrow bb, cc, ss, gg$
 $H \rightarrow inv, H \rightarrow sb, \dots$

Flavor
 CKM matrix
 CPV measurements
 LFV, LUV
 τ properties (lifetime, BRs..)
 $B_c \rightarrow \tau \nu, B_s \rightarrow D_s K/\pi$
 $B_s \rightarrow K^* \tau \tau, B \rightarrow K^* \nu \nu$
 $B_s \rightarrow \phi \nu \nu \dots$

Superior impact parameter resolution for vertices, tagging;
Energy resolution for π^0 or γ reco;
PID: K/ π separation over wide momentum range for b and τ physics

Top
 $m_{top}, \Gamma_{top},$
 top quark coupling,
 ...

~ 4.3 million Higgs
 ~ 4 trillion Z bosons
 ~ 400 million W pairs
 ~ 600 k ttbar

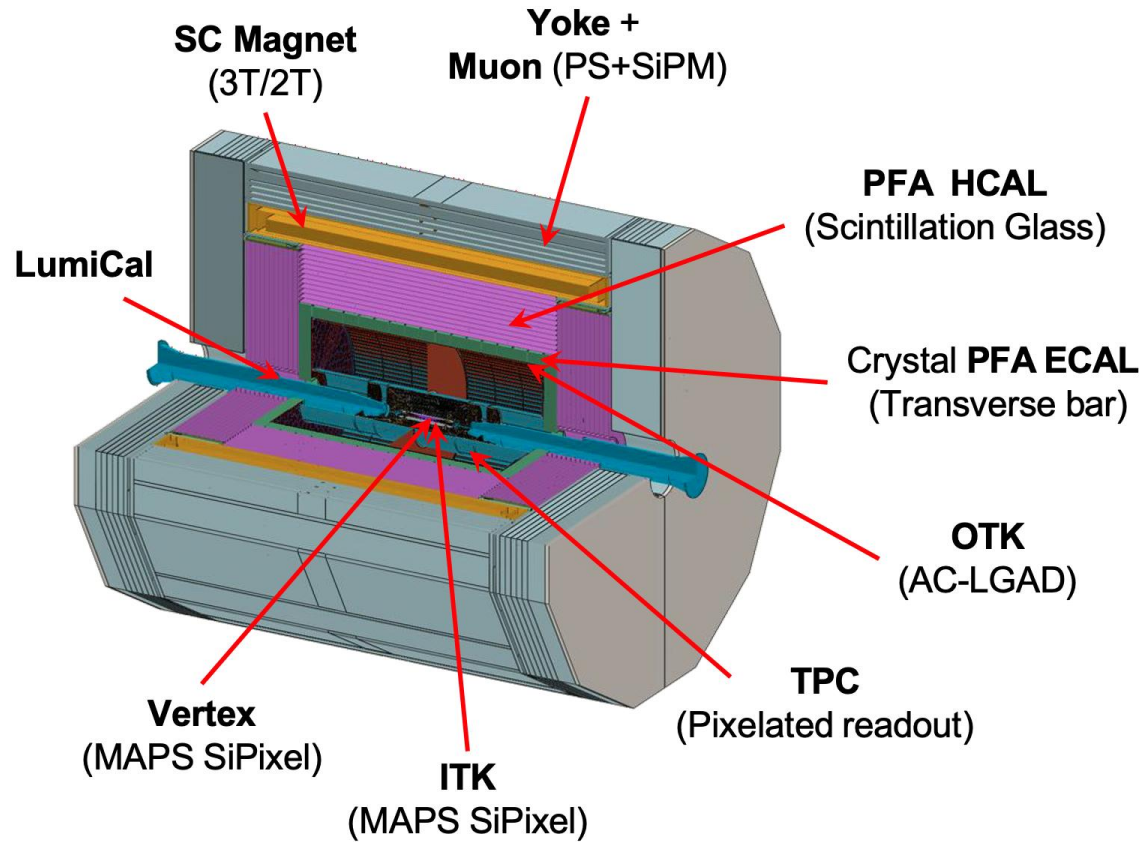
BSM
 Heavy Neutral Leptons
 Dark Photons Z_D
 Axion Like Particles
 Exotic Higgs decays
 ...

LLP sensitivity via far detached vertices (mm \rightarrow m):
Tracking, Calorimetry, Muon

EWK/QCD
 $m_Z, \Gamma_Z, \Gamma_{inv}$
 $\sin^2\theta_W, m_W, \Gamma_W,$
 $A_{FB}^{b,c}, \tau$ pol.
 α_S, \dots

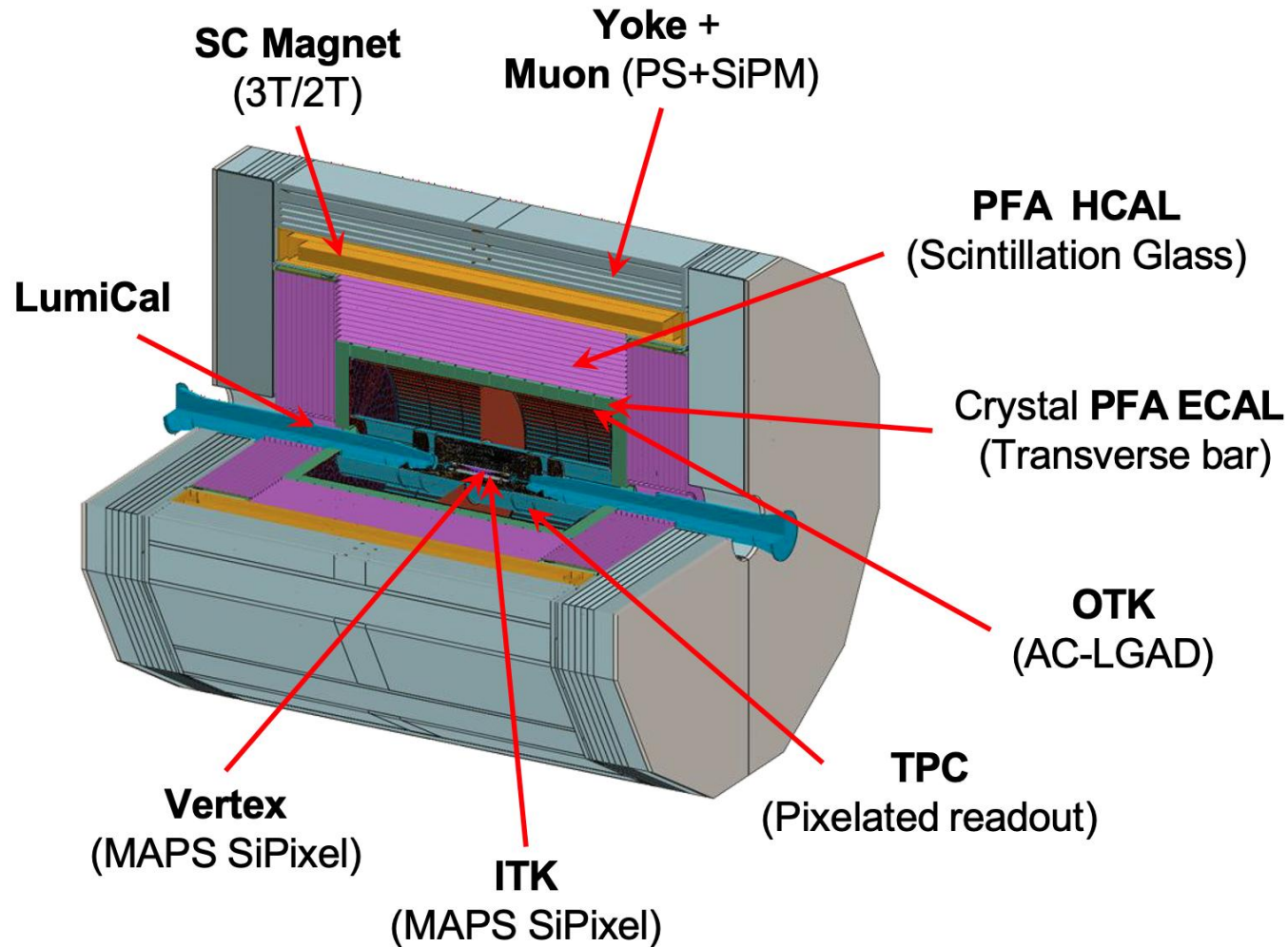
Small systematics:
Absolute normalisation (luminosity, 10^{-4})

Reference Detector Concept



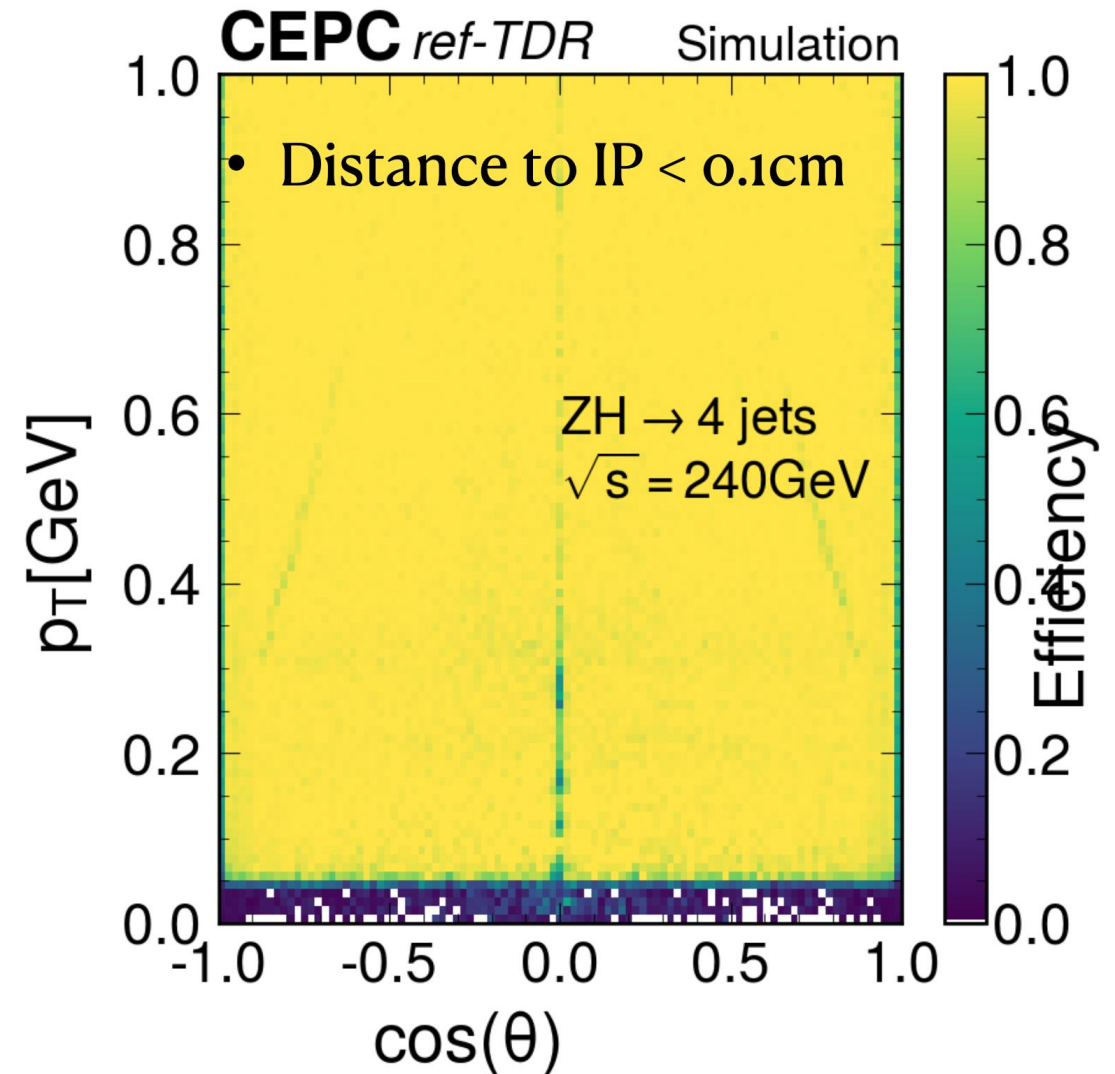
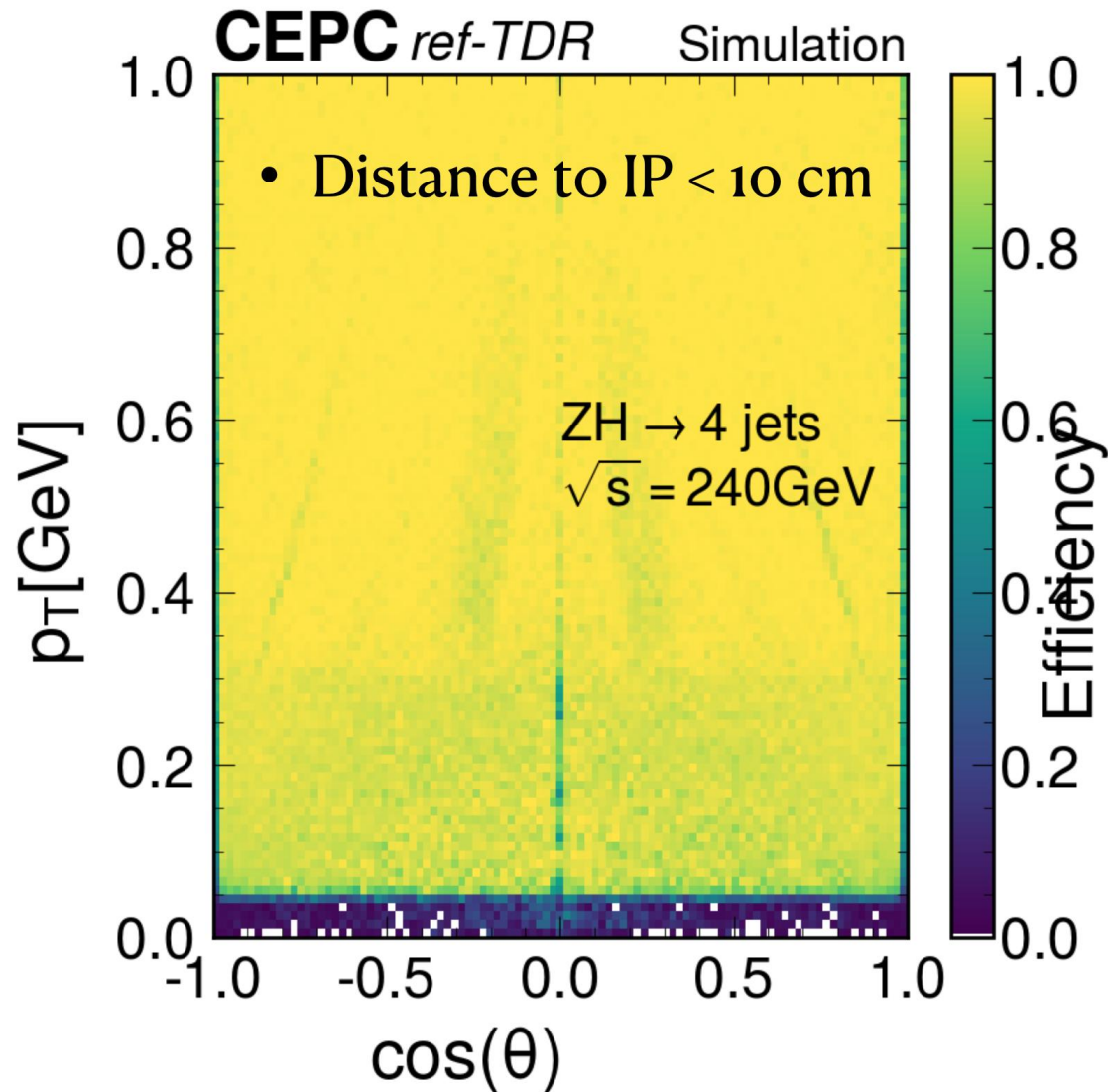
- Ultra-low-mass vertex detector**: four inner layers utilize 65 nm large-area single-layer **stitched sensors**, with the innermost detector radius reaching **11 mm**, + a double-layer ladder structure.
- ITK**: based on **monolithic HV-CMOS pixel sensors**, 3 barrel layers and 4 disk layers at each endcap, **$\sim 20 \text{ m}^2$** .
- TPC**: **pixelated readout, $500 \times 500 \mu\text{m}^2$**
- OTK**: one barrel layer and two endcap disk layers, based on **AC-LGAD to measure timing and position**
- PFA-oriented calorimetry**: **high-granularity homogeneous crystal ECAL** and **novel glass scintillator HCAL**
 - ECAL: 18 longitudinal layers, $\sim 24 X_0$. 40 cm long BGO bars arranged orthogonally in every two adjacent layers. Transverse dimension: **$15 \times 15 \text{ mm}^2$**
 - HCAL: 48 layers of glass scintillator tiles ($4 \times 4 \times 1 \text{ cm}^3$) interspersed with steel plates, $\sim 6 \lambda_I$.
- Superconducting solenoid** \rightarrow **3 T** magnetic field.
- Muon** detectors in the return yoke.
- LumiCal**: an **AC-LGAD silicon** wafer layer and a calorimeter utilizing **LYSO** crystals.

Baseline Detector

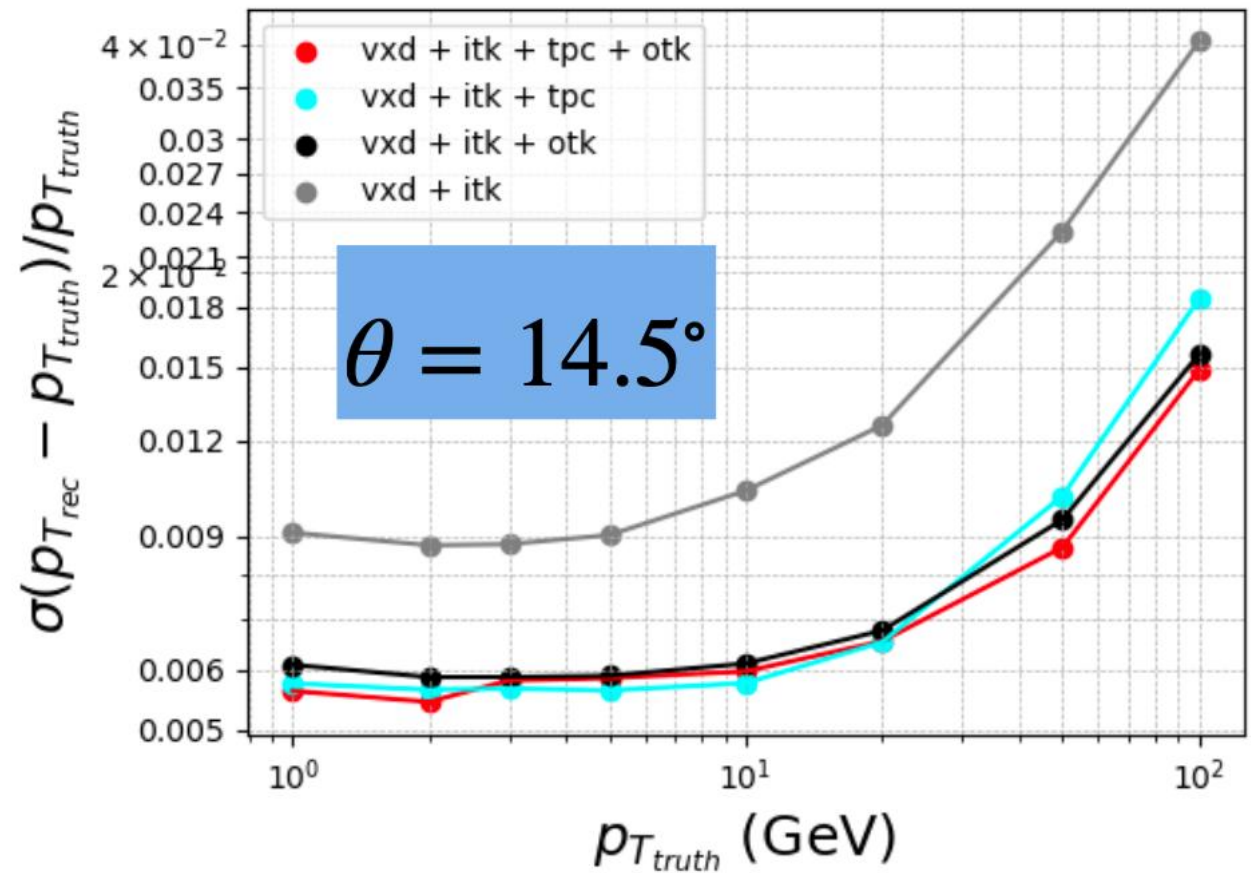
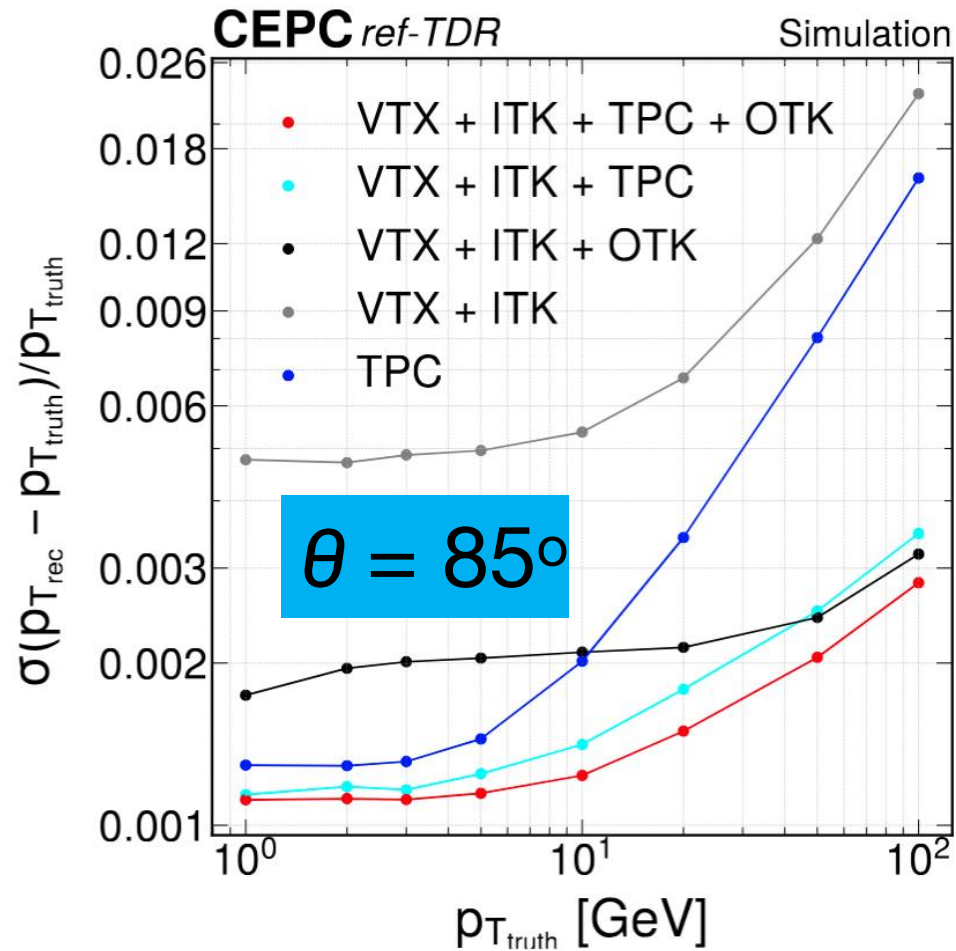


System	Technologies
	Baseline
BeamPipe	ϕ 20 mm
LumiCal	SiTrk + Crystal
Vertex	CMOS + Stitching
Tracker	CMOS Si Pixel ITK
	Pixelated TPC
	AC-LGAD OTK
ECAL	4D Crystal Bar
HCAL	GS+SiPM+Fe
Magnet	LTS
Muon	PS bar+SiPM
TDAQ	Conventional
BE electr.	Common

Some inefficiencies due to Off-IP tracks



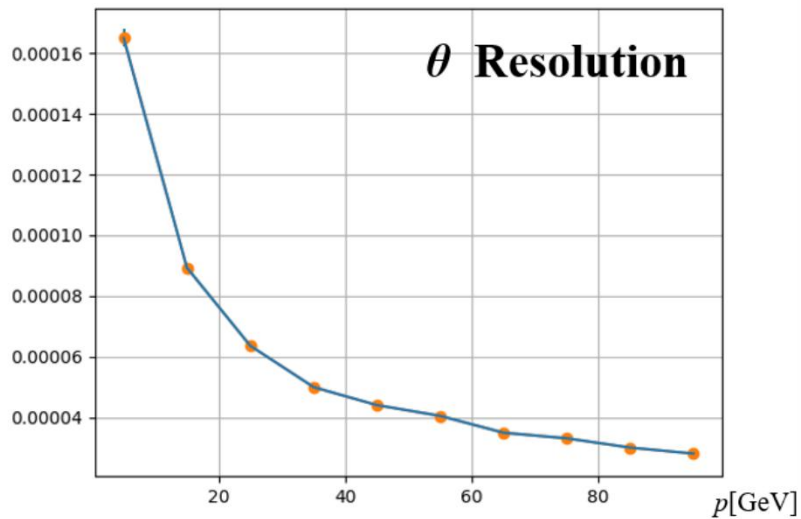
Tracking momentum resolution



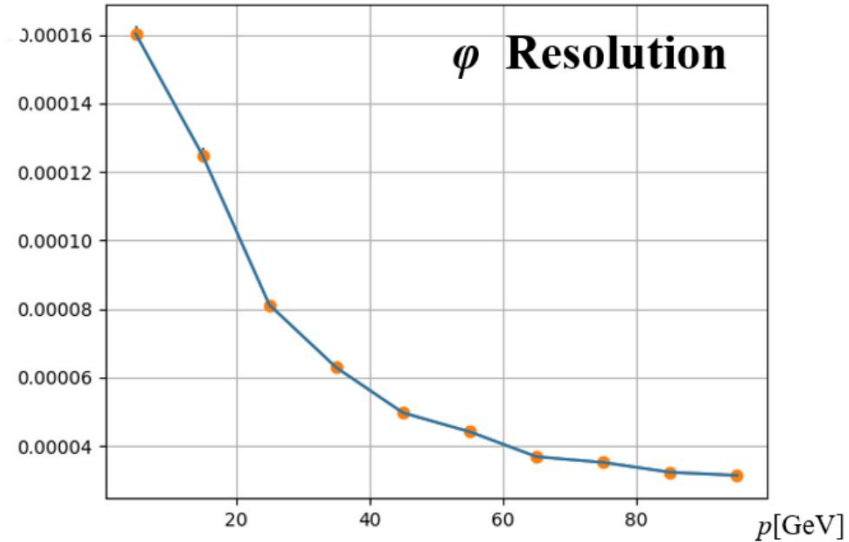
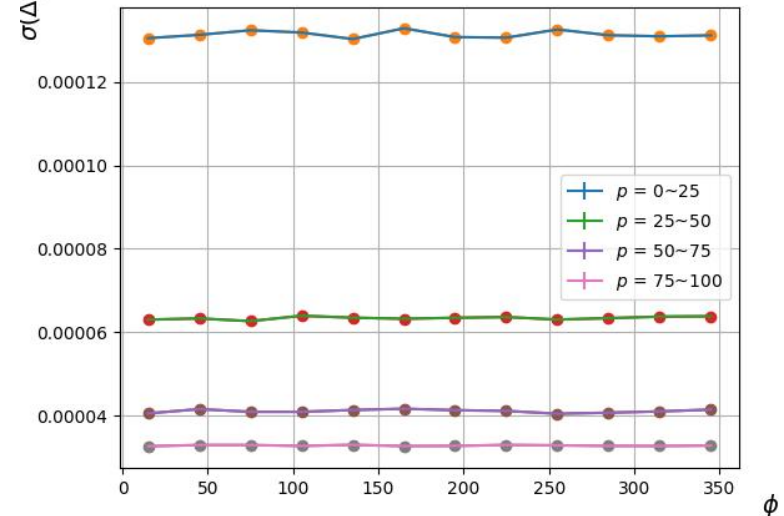
Tracking angular resolution

 $\sigma(\theta)$ [rad]

θ Resolution


 $\sigma(\phi)$ [rad]

ϕ Resolution

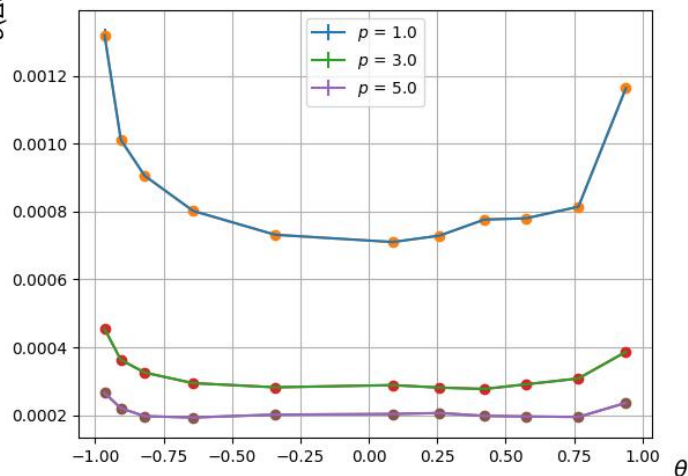
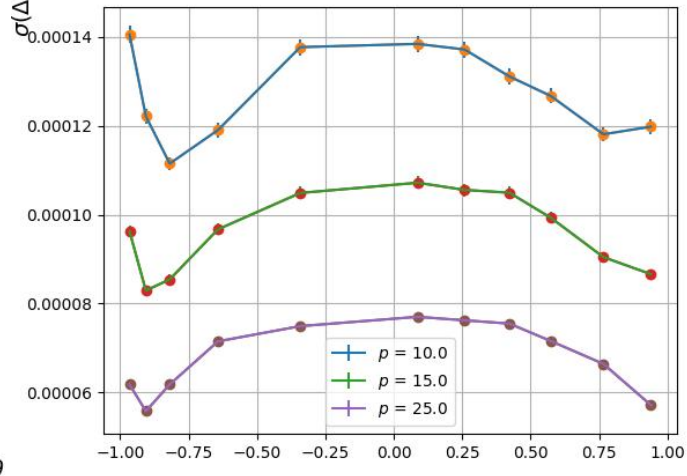
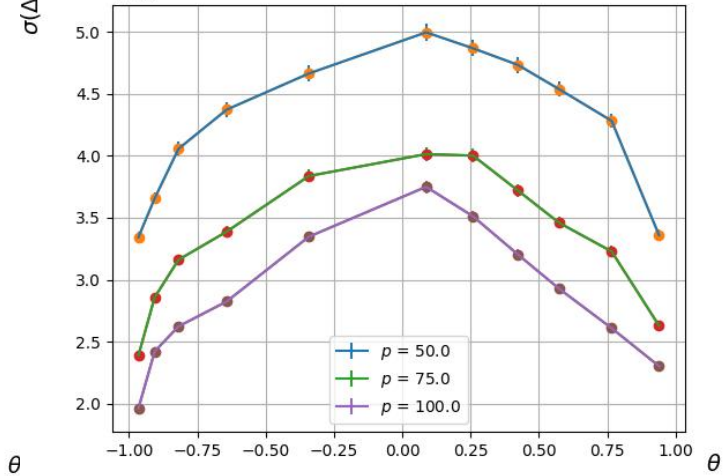

 $\sigma(\Delta\phi)$


$$\Delta\theta|_{res.} = \frac{\sigma_z \sin^2 \theta}{L_0} \sqrt{\frac{12N}{(N+1)(N+2)}}$$

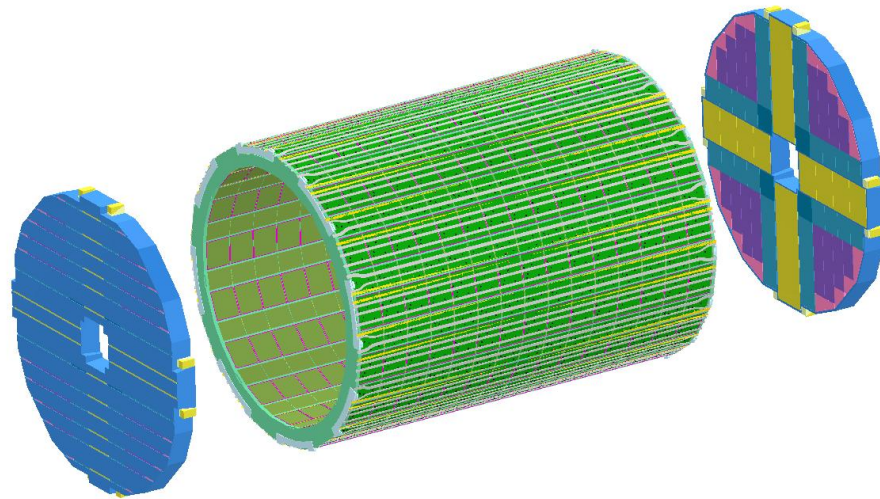
$$\approx \frac{2\sigma_z \sin^2 \theta}{L_0} \sqrt{\frac{3}{N+3}}$$

$$\Delta\theta|_{m.s.} = \frac{\sin \theta}{\beta p_T} f \left(\frac{d}{X_0 \sin \theta} \right)$$

$$\approx \frac{0.0136 \text{ GeV}/c \sin \theta}{\beta p_T} \sqrt{\frac{d}{X_0 \sin \theta}}$$

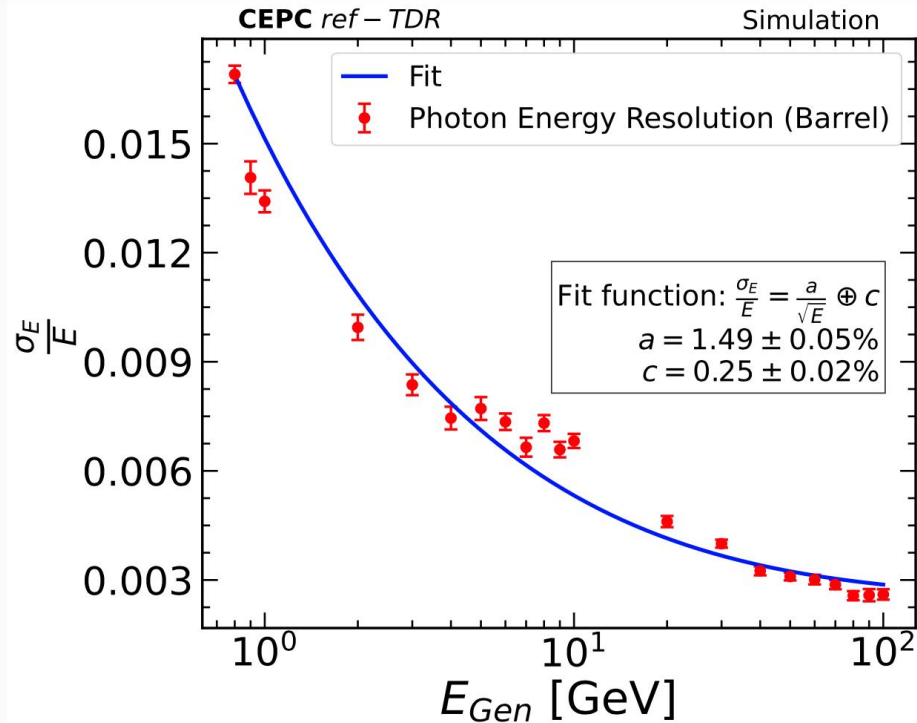
 $\sigma(\Delta\theta)$

 $\sigma(\Delta\theta)$

 $\sigma(\Delta\theta)$


Photon

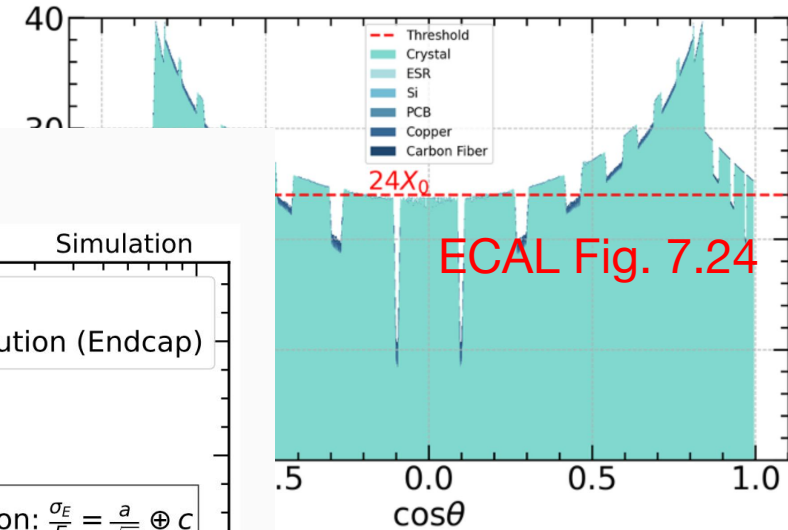
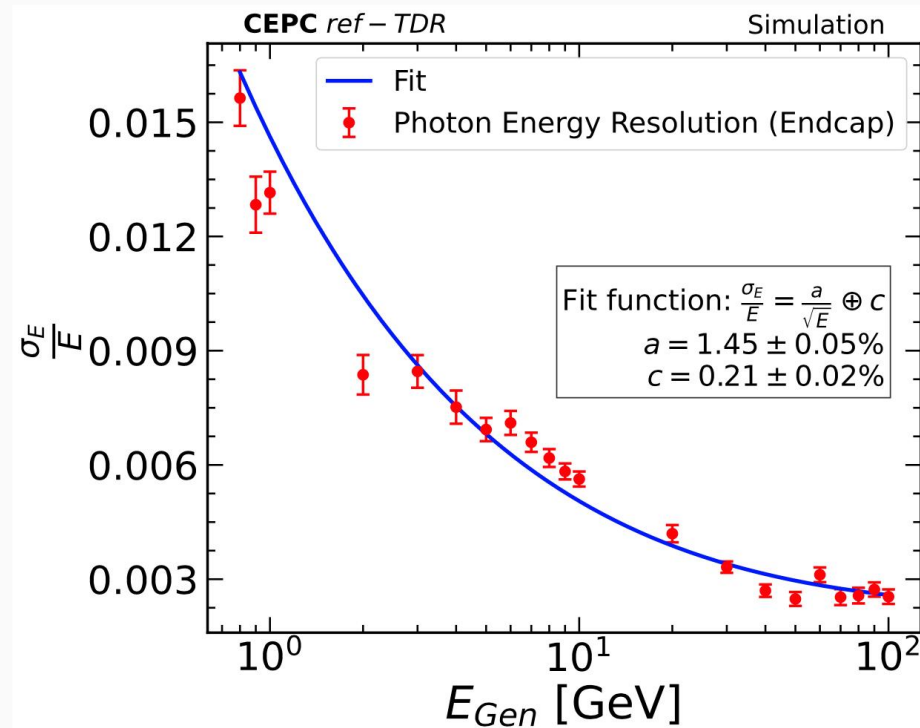


Photon energy resolution

In the barrel:



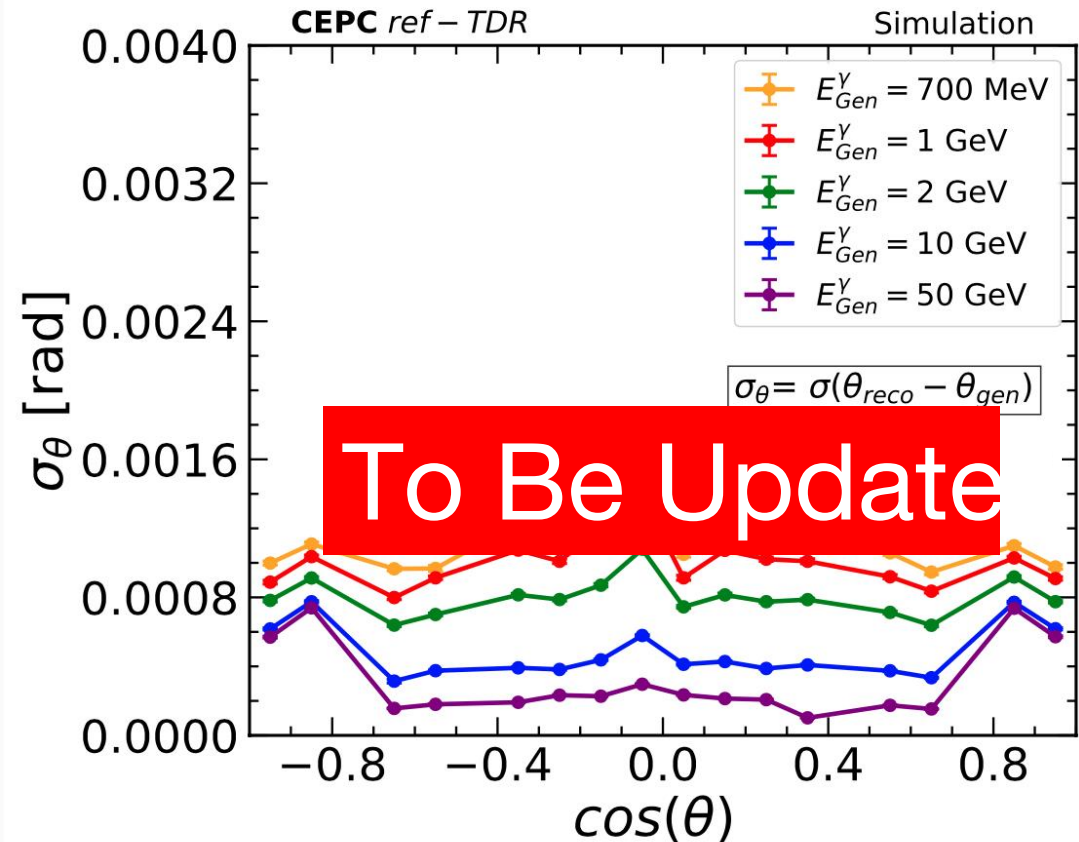
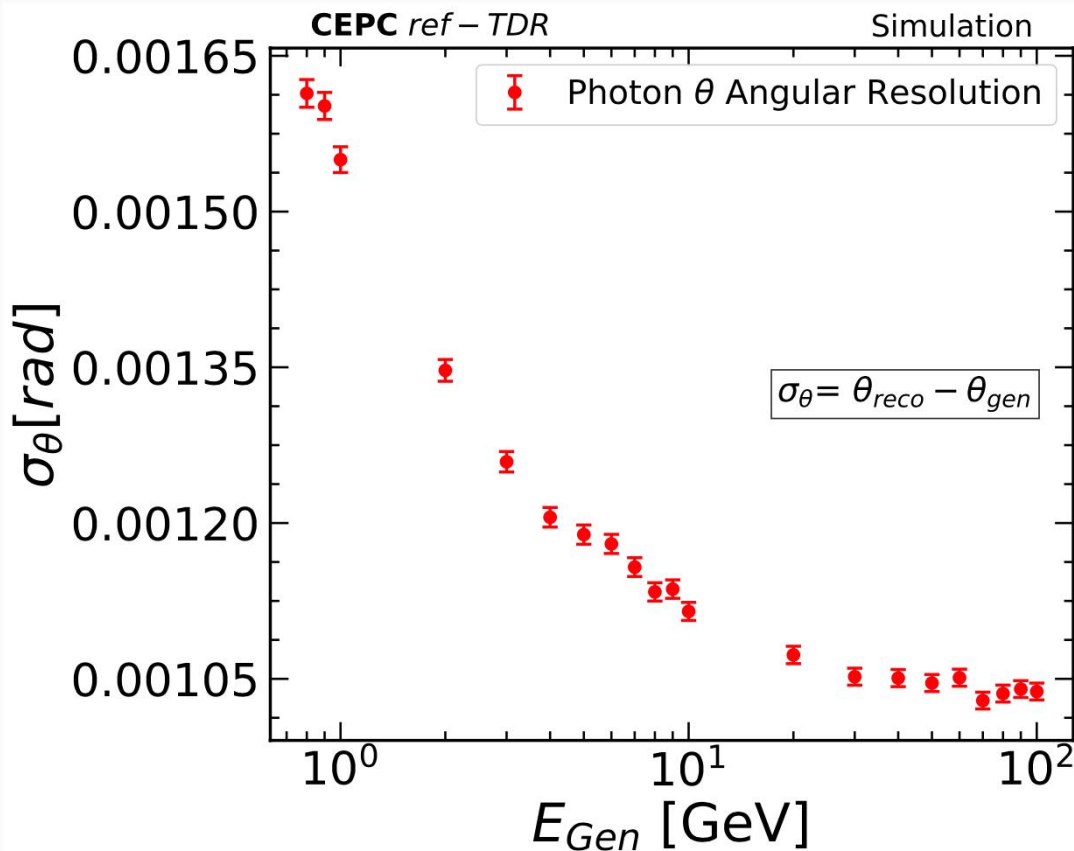
In the endcap:



Few discrepancies for points not fitted well due to the gaps impact (dead material alongside both θ and Φ)

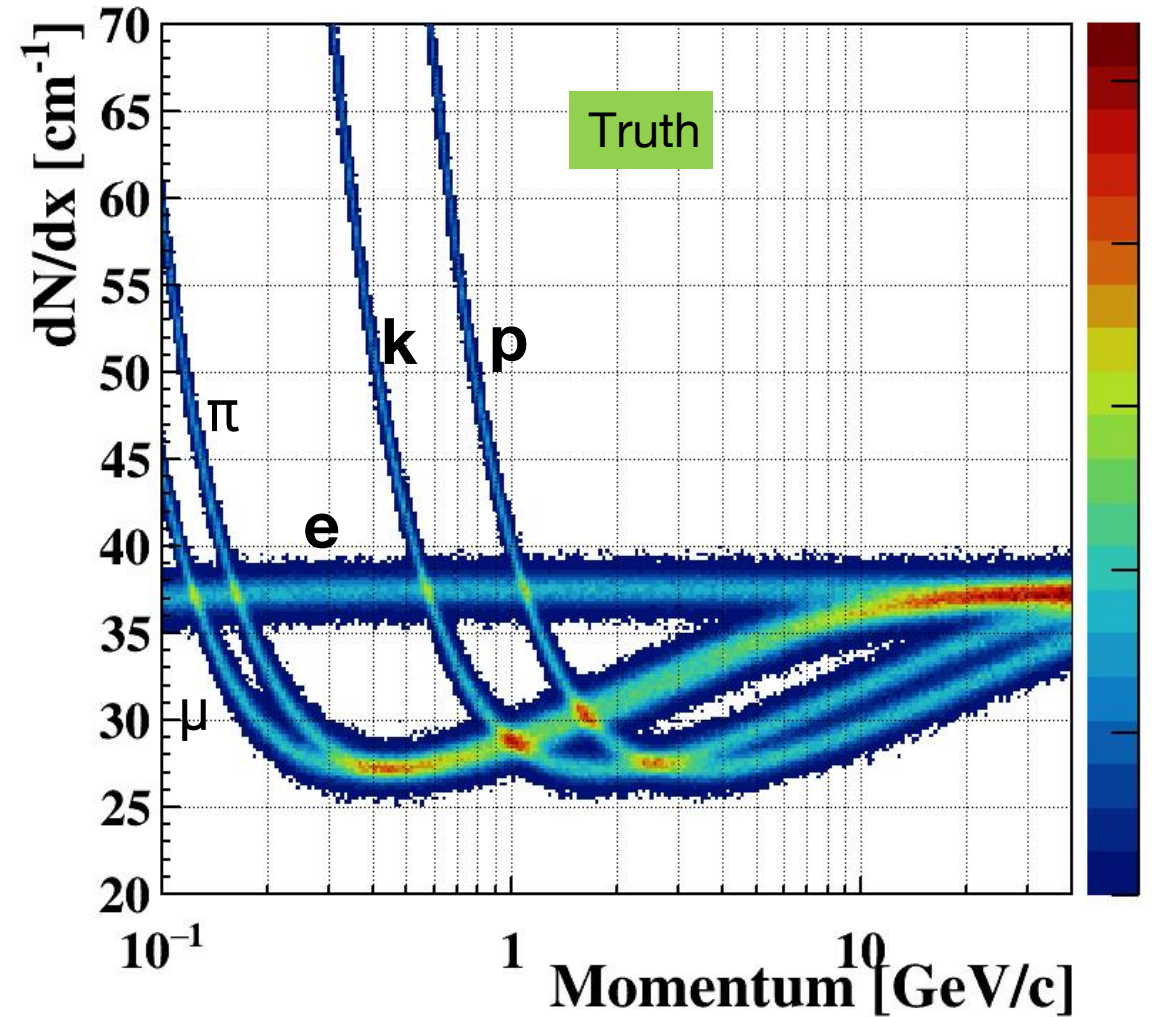
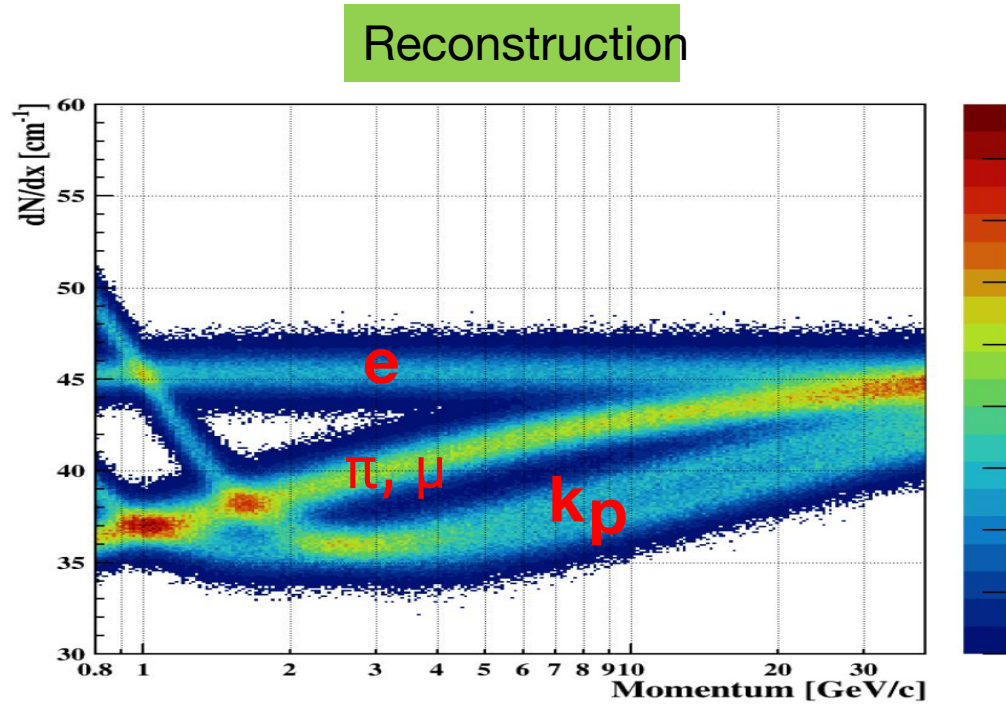
Endcap results similar to barrel: only γ entering ECAL after shower used for fitting, resolution not related to amount of material in front of the Endcap.

Photon Angular Resolution Not in TDR

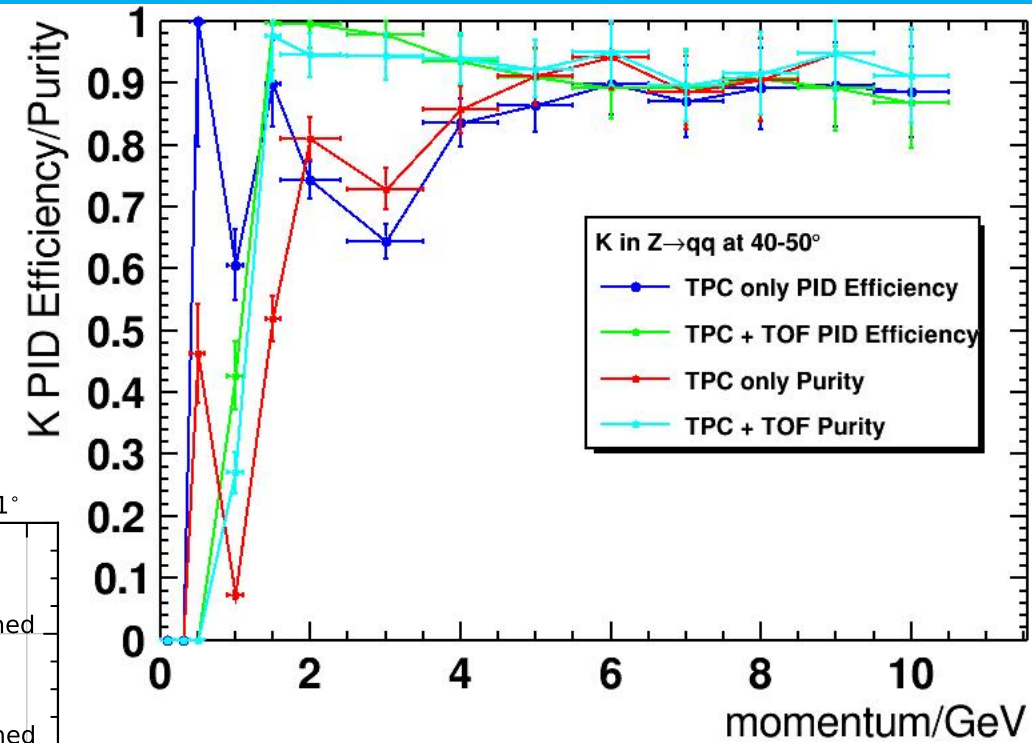
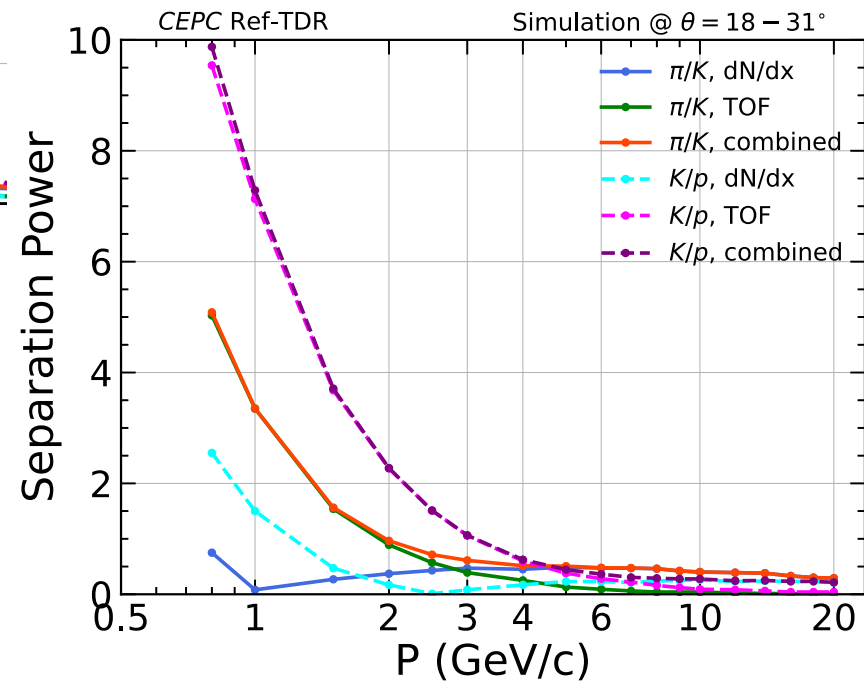
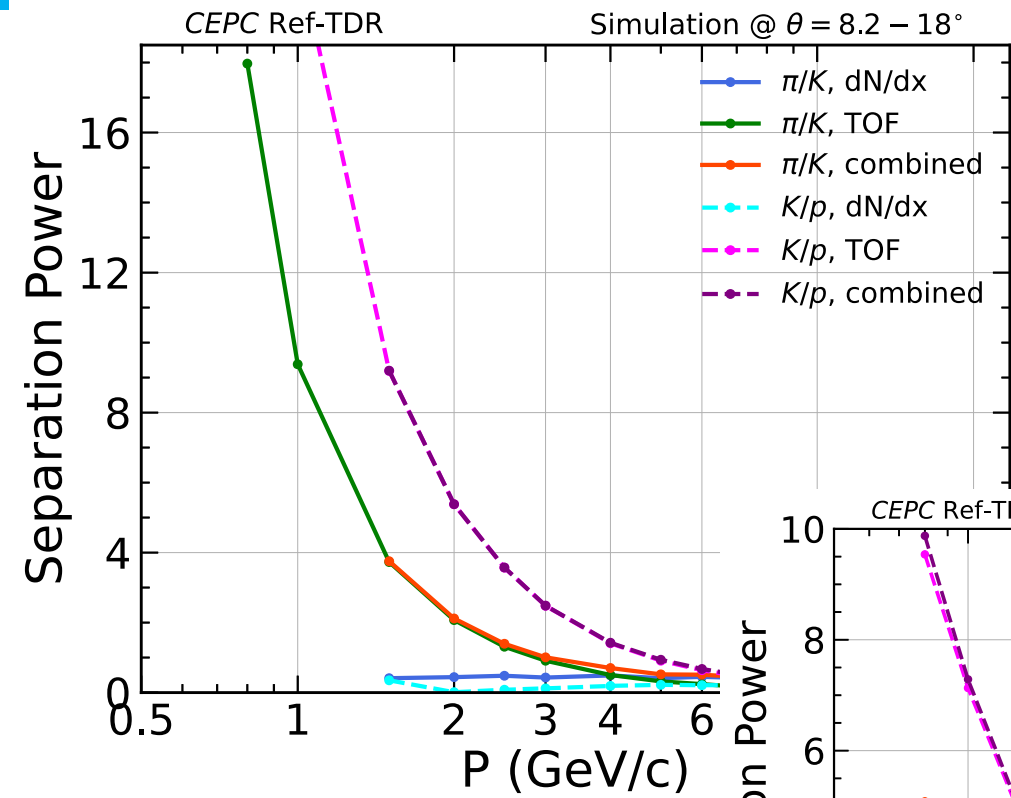


- Photon θ angular resolution slightly worse than expectation: around 0.045° or 0.000785 rad (approximation from ECAL shower position reso. around $1/10 * 15\text{mm} = 1.5\text{mm}$)

Charged Hadron PID – TPC



Charged Hadrons



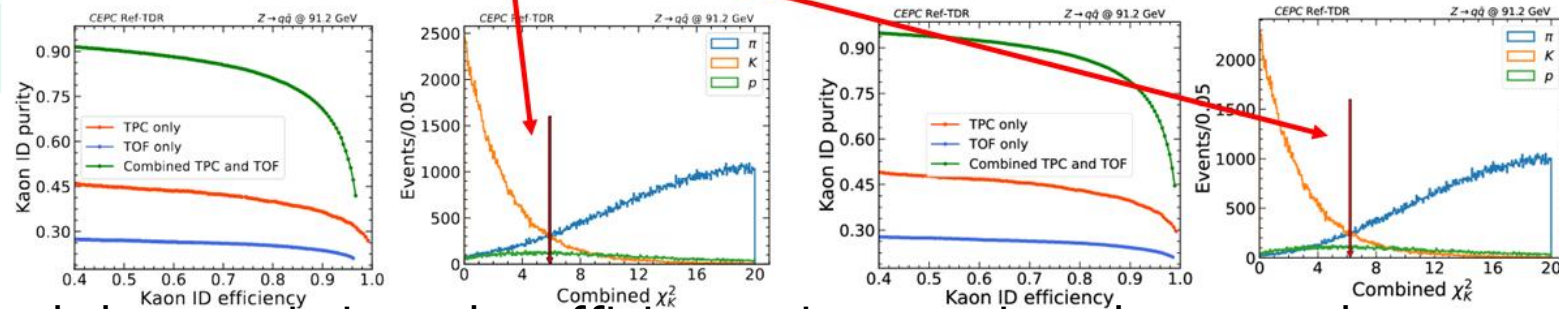
Kaon eff vs. purity

Kaon Track

Z → q \bar{q} 100000 events (truth MCParticle charged stable e, μ , π , K, p: 2288676)				
Track selection criteria		Ntrack	Absolute Efficiency	Relative Efficiency
(a) CompleteTracks	...	2268408	100%	100%
(b) Track-MCP Match : CompleteTracks ParticleAssociation	Track hits match with stable MCParticle Choose MCParticle with max weight as truth particle	2268408	100%	100%
	Match with charged e, μ , π , K, p	2184944	96.32%	96.32%
	Match with charged K	230785	10.17%	10.56%
(c) No decays	Veto isdecayintrker	169639	7.48%	73.51%
(d) Hit TPC	matchedtpc	157234	6.93%	92.69%
(e) Hit TOF	matchedtof	141891	6.26%	90.24%
(f) No daughters	daughtersize==0	137638	6.07%	97.00%
(g) Track fitting	$\chi^2/ndof < 2$	136439	6.01%	99.13%
(h) Veto regions	Not in (p<0.5GeV && cos θ < 0.55) (p<1GeV && cos θ > 0.55) (p>4GeV && cos θ > 0.9)	128872	5.68%	94.45%

Kaon PID

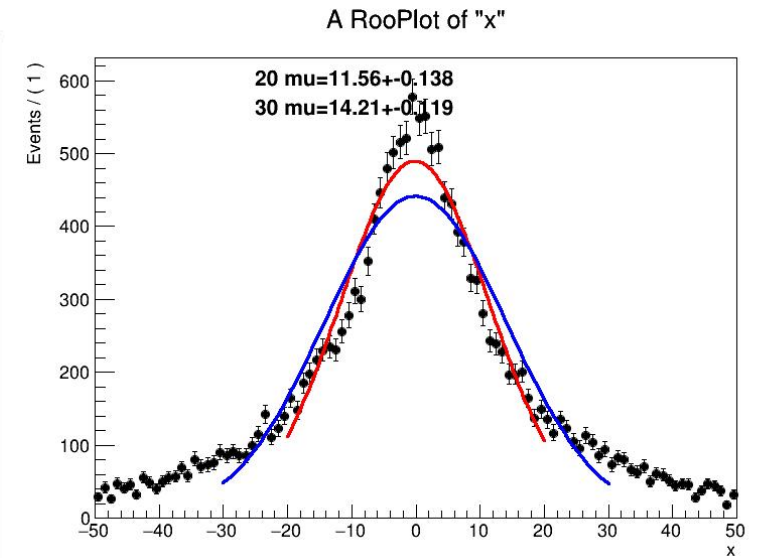
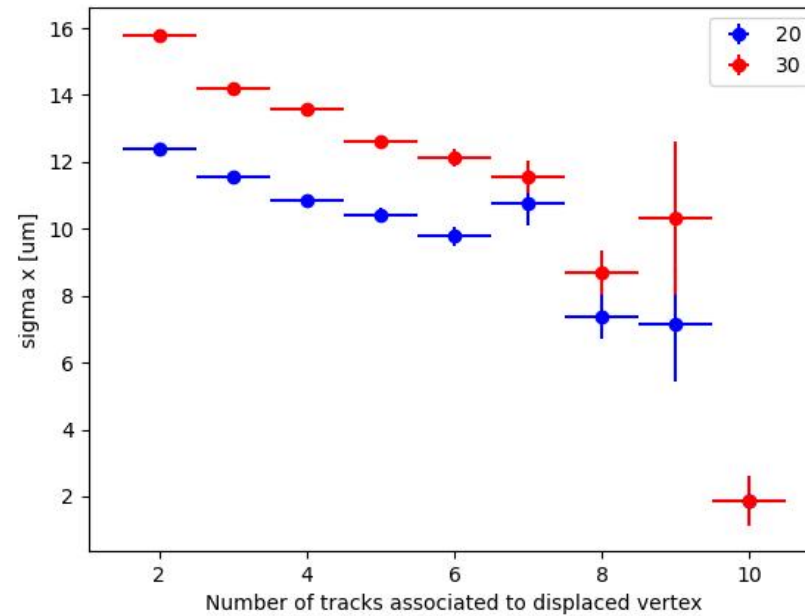
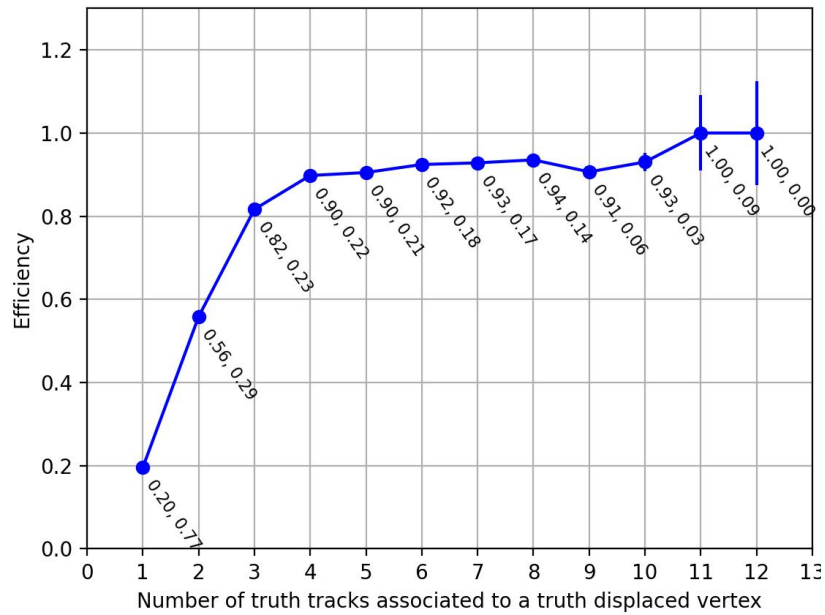
Kaon PID Efficiency just among charged π, K, p							
Selections	K Ntrack	PID Strategy	K to K Ntrack	PID Eff.	π, K, p to K Ntrack	Purity	Eff*Purity
(a)-(e)	141891	Combined χ_K^2 be the minimum	124627	87.83%	153255	81.32%	71.43%
		Maximize Kaon PID eff*purity Combined $\chi_K^2 < 5.886$	119230	84.03%	152693	78.08%	65.61%
(a)-(h)	128872	Combined χ_K^2 be the minimum	117213	90.95%	135181	86.71%	78.86%
		Maximize Kaon PID eff*purity Combined $\chi_K^2 < 6.217$	112700	87.45%	137871	81.74%	71.49%



By applying the cut on the χ^2_{Combined} that maximizes the efficiency times purity, shown as the downward arrow in Figure 15.11 (right), the kaon identification efficiency and purity can reach 87.4% and 81.7%, respectively (Note that here the cut is not optimized bin by bin).

Secondary Vertex

Zbb sample



Physics level: without event cleaning

Detector level: with event cleaning

$|Pt_{isr}|, |Pt_v| < 1\text{ GeV}$. $|\cos\theta_{jet}| < 0.85$ in the table.

BMR

25.1.0

Case	process	$ZH \rightarrow \nu\nu gg$	$ZH \rightarrow \nu\nu bb$	$ZH \rightarrow \nu\nu cc$	$ZH \rightarrow \nu\nu uu$	$ZH \rightarrow \nu\nu dd$	$ZH \rightarrow \nu\nu ss$
Physical level	BMR/%	4.00 ± 0.01	4.36 ± 0.03	4.16 ± 0.03	3.79 ± 0.01	3.97 ± 0.01	4.44 ± 0.01
	Efficiency/%	73.3	73.7	74.0	74.2	74.1	74.1
Detector level	BMR/%	3.95 ± 0.01	3.74 ± 0.02	4.01 ± 0.01	3.77 ± 0.01	3.95 ± 0.01	4.40 ± 0.01
	Efficiency/%	65.7	28.1	48.6	70.3	70.1	70.2

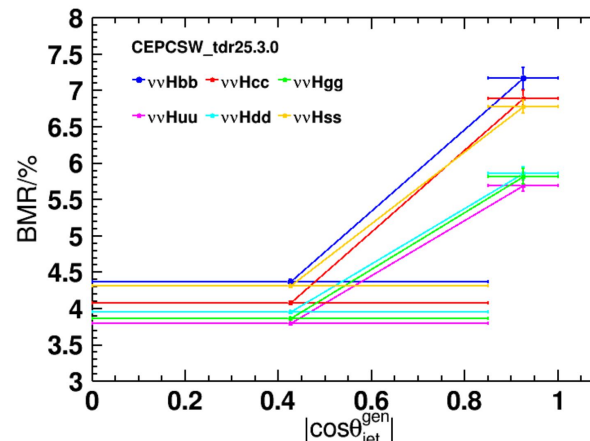
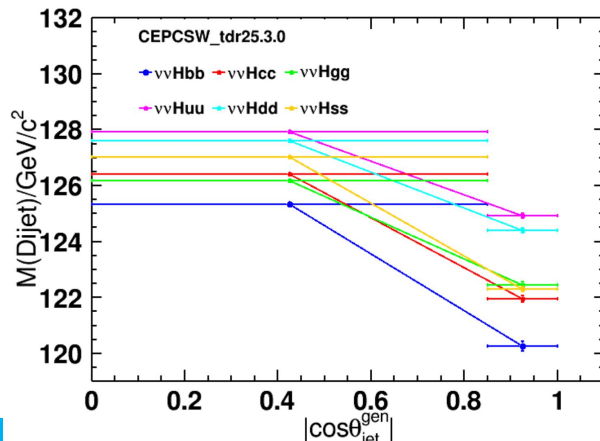
25.3.0

Case	process	$ZH \rightarrow \nu\nu gg$	$ZH \rightarrow \nu\nu bb$	$ZH \rightarrow \nu\nu cc$	$ZH \rightarrow \nu\nu uu$	$ZH \rightarrow \nu\nu dd$	$ZH \rightarrow \nu\nu ss$
Physical level	BMR/%	3.87 ± 0.01	4.37 ± 0.03	4.09 ± 0.02	3.82 ± 0.01	3.97 ± 0.01	4.33 ± 0.01
	Efficiency/%	74.4	74.5	74.8	74.9	74.8	74.8
Detector level	BMR/%	3.82 ± 0.01	3.70 ± 0.01	3.92 ± 0.01	3.80 ± 0.01	3.94 ± 0.01	4.30 ± 0.01
	Efficiency/%	66.7	28.4	49.1	71.2	70.8	70.9

Observation:

better BMR in 25.3.0 with 15mm x 15mm crystal bar geometry than 10x10 in 25.1

Should be due to the improved PFA clustering



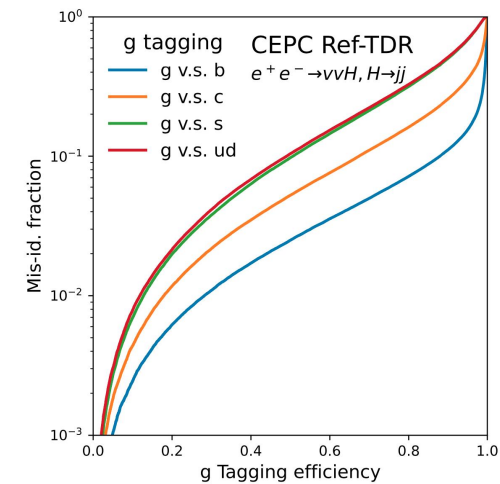
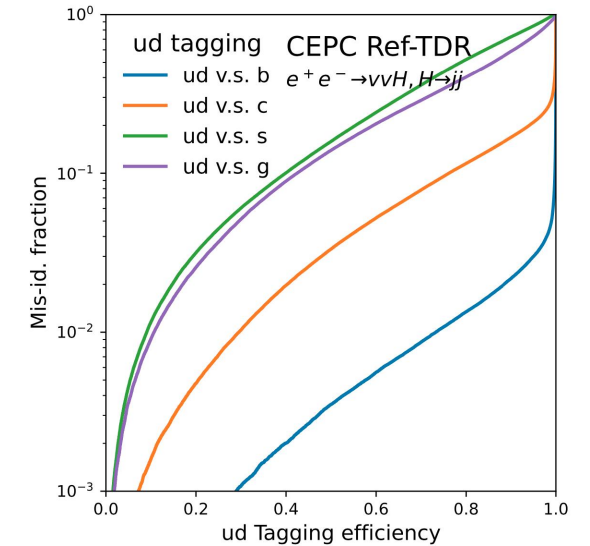
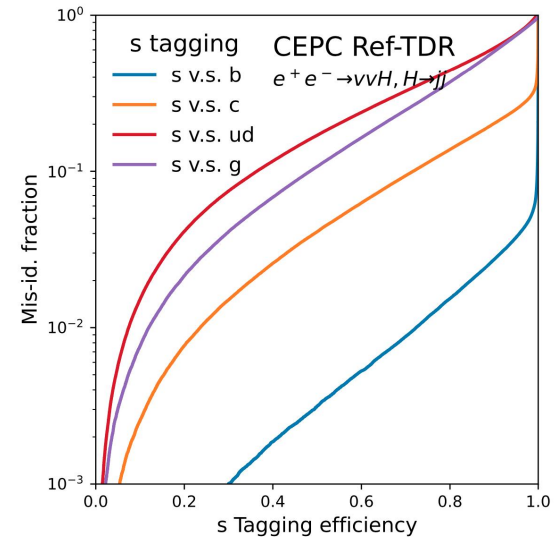
Dijet mass and BMR of barrel and endcap

Much worse resolution in endcap as expected

Jet Origin ID (JOI)

tdr, reco pid

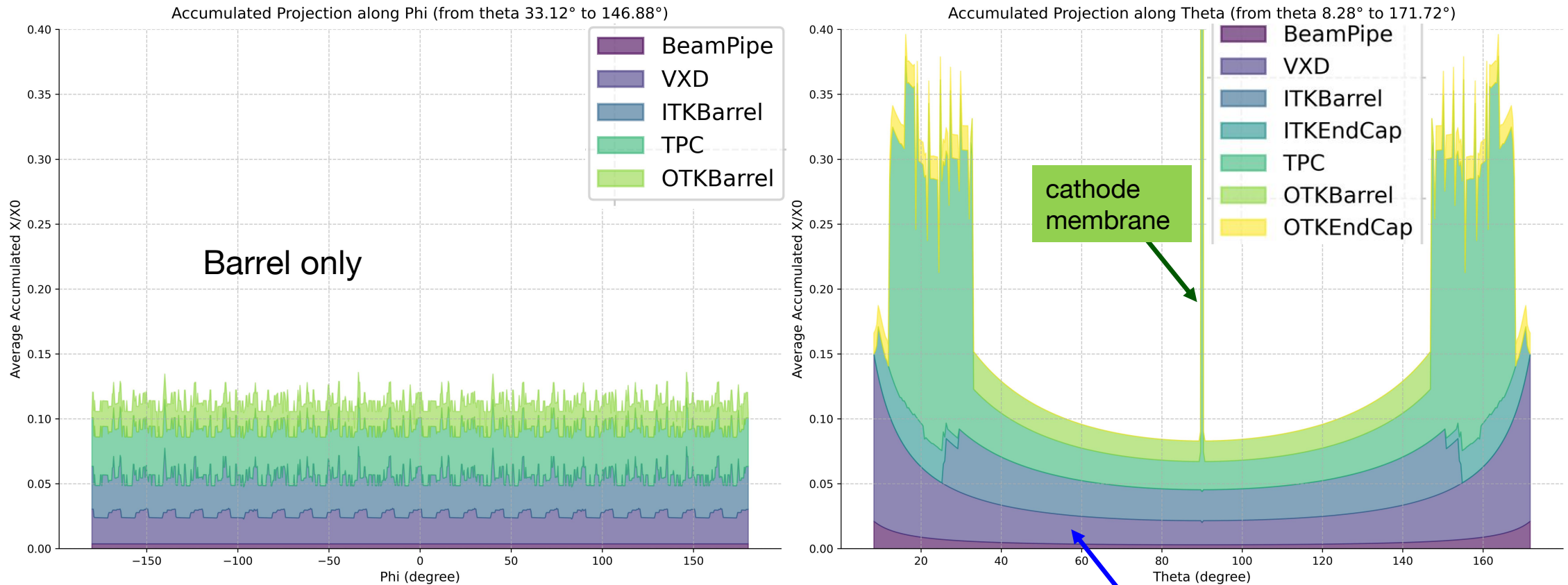
True \ Predicted	b	\bar{b}	c	\bar{c}	s	\bar{s}	u	\bar{u}	d	\bar{d}	g
b	0.7566	0.1523	0.0256	0.0285	0.0039	0.0026	0.0018	0.0032	0.0021	0.0012	0.0222
\bar{b}	0.1582	0.75	0.0281	0.0264	0.0029	0.0038	0.0032	0.0015	0.0014	0.0019	0.0226
c	0.0127	0.0155	0.7199	0.0607	0.0294	0.0372	0.032	0.0071	0.0088	0.0206	0.056
\bar{c}	0.0169	0.0114	0.0566	0.7261	0.0379	0.0276	0.0076	0.0324	0.0202	0.0085	0.0548
s	0.0024	0.0016	0.019	0.0254	0.4772	0.0974	0.0231	0.1219	0.0736	0.0492	0.1093
\bar{s}	0.0018	0.0022	0.025	0.0195	0.1016	0.4736	0.1196	0.0241	0.0504	0.0729	0.1092
u	0.0015	0.0024	0.0268	0.0119	0.0463	0.1771	0.3597	0.0377	0.0665	0.1527	0.1175
\bar{u}	0.0023	0.0016	0.0108	0.0268	0.1751	0.0453	0.0383	0.3579	0.1629	0.0614	0.1177
d	0.0023	0.0016	0.0134	0.0274	0.1533	0.0956	0.0549	0.23	0.2285	0.0726	0.1205
\bar{d}	0.0018	0.0024	0.026	0.0136	0.1005	0.1501	0.2326	0.055	0.0792	0.2169	0.1221
g	0.016	0.015	0.0344	0.0354	0.0826	0.0812	0.0641	0.0641	0.0463	0.0444	0.5164



Material Budget

Not in TDR

Detector Material Budget Accumulation Analysis for CEPC tdr25.3.7



- Supporting material (carbon fiber) for beampipe in the current SW much more than expected
 - 2.5 mm thickness (1.8% X_0) instead of the actual design 1.5 mm (mis-counted in VXD. to be separated)
 - Expect further improvement on tracking resolution** (material budget reduced by 0.7% X_0)

Jet Flavor Tagging with XGBoost BDT

Table 15.1: BDT input variables for jet tagging

Name	Description
VtxLxyz	Decay length of the vertex.
VtxLxyzSig	Significance of the decay length (calculated using the covariance matrix).
VtxMomenta	Magnitude of the momenta of all tracks forming the vertex.
VtxEnergy	Sum of the track energies of the vertex.
VtxMass	Mass of the vertex, calculated using the tracks' four-momentum.
VtxAngle	Angle between the vertex position direction and the total track momentum.
VtxCollinearity	Collinearity between vertex position direction and the total track momentum.
VtxNtrk	Number of tracks forming the vertex.
VtxChi2	Chi-square of the vertex fitting.
VtxNumber	The number of vertices reconstructed in the jet.
VtxTotalTrk	Total number of tracks forming all vertices in the jet.
VtxTotalMass	Total mass of all vertices, computed as the sum of all tracks' four-momenta.
VtxDistance	Distance between the first two vertices.
VtxDistanceSig	Significance of the distance between the first two vertices.
SingleVtxProb	Vertex probability with all associated tracks combined.
MultiVtxProb	For multiple vertices, the probability P is computed as $1 - P = (1 - P_1)(1 - P_2)(1 - P_3) \dots$
TrkTotalMass	Total mass of all tracks exceeding 5σ significance in d_0/z_0 values.
TrkTotalD0Prob	Product of the d_0 probabilities of all tracks under the b/c/uds-quark hypotheses using the corresponding d_0 distributions.
TrkTotalZ0Prob	Product of the z_0 probabilities of all tracks under the b/c/uds-quark hypotheses using the corresponding z_0 distributions.
TrkD0Sig	d_0 significance of the two tracks with the highest d_0 significance.
TrkZ0Sig	z_0 significance of the two tracks with the highest d_0 significance.
TrkPt	Transverse momentum of the two tracks with the highest d_0 significance.

- XGBoost classifier employed
- Similar set of variables used as in the LCFIPlus paper [arXiv:1506.08371](https://arxiv.org/abs/1506.08371)